Renewable Hydrogen Technologies: Production, Purification, Storage, Applications and Safety

Chapter 18: Update on the progress of hydrogen-fueled internal combustion engines

Abstract

This chapter provides an overview on the use of hydrogen as a fuel for internal combustion engines. First, pros and cons are discussed for using hydrogen to fuel internal combustion engines versus fuel cells. Then, the properties of hydrogen pertinent to engine operation are briefly reviewed, after which the present state-of-the-art of hydrogen engines is discussed. Ongoing research efforts are highlighted next, which primarily aim at maximizing engine efficiency throughout the load range, while keeping emissions at ultra-low levels. Finally, the challenges for reaching these goals and translating lab results to production are discussed.

Keywords

Hydrogen, internal combustion engine, efficiency, port fuel injection, direct injection, transportation, vehicles, sustainable

Introduction

H_2-ICE vs. fuel cell

The interest in hydrogen as an energy carrier or buffer is explained in detail throughout this book. A lot of research effort has gone into the development of the hydrogen-fueled fuel cells for stationary or transport applications as also discussed elsewhere. Fuel cells are attractive for their high efficiency potential throughout the load range with their high efficiency at part

load operation being of particular interest to transportation applications. Furthermore, they are relatively quiet and only emit water vapor as the reaction product. Much less attention has been devoted to internal combustion engines (ICEs) using hydrogen as fuel. The ICE is often readily dismissed as a future prime mover, for its low efficiency (particularly at part load), and pollutant emissions. However, as discussed in this chapter, because of hydrogen's unique properties, it is possible to substantially increase the ICE's efficiency when operated on hydrogen. When using high temperature oxidation of fuel to produce power, i.e. combustion, the formation of oxides of nitrogen (NO and NO_2, collectively termed NO_X) is possible, which is a disadvantage compared to the low temperature oxidation in fuel cells. Again, the unique properties of hydrogen allow the emission of NO_X to be ultra-low if adequate measures are taken, as explained below.

More importantly, ICEs have the very interesting feature of being able to operate on different fuels. This "flex-fuel" ability is an advantage for introducing hydrogen vehicles to the marketplace. First, this can assist with the gradual build-up of a hydrogen fueling infrastructure, and secondly, this can alleviate the on-board storage challenge, with a second fuel (e.g. gasoline) essentially serving as a "range extender". The much lower cost of a hydrogen-fueled ICE compared to a fuel cell is another advantage that can help with setting up demonstration fleets etc., with the HyNor project vehicle fleet being a prime example (see http://hynor.no). The lower cost not only applies to the ICE itself, but also to the fuel: the ICE can handle lower purity hydrogen without any problems.

The hydrogen-fueled ICE has thus been recognized as being a compelling bridging technology to introduce hydrogen as an energy carrier for transportation [1]. However, it has also been advanced as a sustainable and scalable technology, as the ICE is made from abundantly available and recyclable materials [2], which might not be the case for fuel cells, that require relatively large amounts of platinum.

In the following, hydrogen's properties as an engine fuel are reviewed, the current state-of-

the-art in hydrogen engines and hydrogen ICE equipped vehicles is presented, the present research on H_2 ICEs is described and an outlook on where the development is headed is given.

H_2 properties relevant for ICE

Since hydrogen is a gas at ambient conditions, its properties are significantly different from conventional liquid fuels. Table 1 shows a comparison of relevant properties of hydrogen, methane (as the main constituent of natural gas) and iso-octane (representative of gasoline fuel). Although some properties of hydrogen, namely laminar flame speed and flammability range, are advantageous for internal combustion engines, other properties pose challenges for the design of a hydrogen-fueled vehicle. As an example, the density of hydrogen at ambient conditions is almost two orders of magnitude lower than methane. This presents a challenge for storing sufficient amounts of the gaseous fuel on-board a vehicle even under compressed or liquefied conditions. The low density also negatively affects the power density of hydrogen engines with external mixture formation.

As far as combustion is concerned, the minimum ignition energy of hydrogen is more than an order of magnitude lower than that of methane or iso-octane suggesting that hydrogen is easy to ignite. While the ignitability decreases with leaner air/fuel mixtures, its low level at stoichiometric conditions presents a challenge due to the occurrence of combustion anomalies at high engine loads. The significantly lower minimum quenching distance results in hydrogen flames to burn closer to the combustion chamber walls potentially decreasing engine efficiency due to increased wall heat losses. The mass-specific lower heating value as well as the stoichiometric air demand of hydrogen is significantly higher than for methane or iso-octane. These two factors in combination with the density determine the mixture calorific value which is discussed in a subsequent section. The flammability limits of hydrogen are extremely wide compared to other fuels and hydrogen is ignitable in a range from 4-75 vol%.

Figure 1 graphically compares the flammability limits of hydrogen to diesel, gasoline and methane. These wide flammability limits are the key to the application of lean-burn combustion strategies with hydrogen as a fuel. Another factor making hydrogen very suitable for lean-burn combustion concepts is the high flame speeds even under lean conditions. Figure 2 compares the laminar flame speeds of stoichiometric hydrogen-, iso-octane- and methane-air mixtures as a function of relative air/fuel ratio λ, defined here as the air/fuel ratio (AFR) relative to the air/fuel ratio in a stoichiometric mixture (AFR_{st}). Relative air/fuel ratio λ, and fuel/air equivalence ratio ϕ, are calculated using the following equations:

$$AFR = \frac{m_{air}}{m_{fuel}} \tag{1}$$

$$AFR_{st} = \left(\frac{m_{air}}{m_{fuel}}\right)_{st} \tag{2}$$

$$\lambda = \frac{AFR}{AFR_{st}} \tag{3}$$

$$\phi = \frac{AFR_{st}}{AFR} \tag{4}$$

Engine combustion is a highly turbulent event with flame speeds that are an order of magnitude higher than the laminar flame speed. Nonetheless the laminar flame speed can be used as an indicator for in-cylinder combustion velocity suggesting extremely short combustion durations for stoichiometric hydrogen-air mixtures. Furthermore, hydrogen-air mixtures at a relative air/fuel ratio λ of 2 still burn about as fast as stoichiometric iso-octane- or methane-air mixtures.

The significance of lean combustion is its positive effect on engine efficiency. Under idealized conditions, the engine efficiency (η) can be estimated based on the engine's compression ratio (r_c) and the isentropic coefficient (γ), which is a function of the air/fuel ratio, using the following equation [7]:

$$\eta = 1 - \frac{1}{r_c^{\gamma-1}} \quad (5)$$

The theoretical engine efficiency can therefore be increased by a lean burn strategy (lean mixtures have higher γ than stoichiometric mixtures), allowed by the wide flammability range of hydrogen.

Another critical property of combustion engine fuels is their resistance to knock, an abnormal combustion event caused by auto-ignition of the end gases resulting in extremely high pressure oscillations. Research and Motor Octane Number (RON and MON) are used to express the resistance of liquid, spark-ignition engine fuels to knocking combustion. While a determination of RON and MON for gaseous fuels is not applicable, research suggests that the knock resistance of hydrogen strongly depends on air/fuel ratio [8]. While stoichiometric mixtures are prone to knock, engines have been operated knock-free under high load conditions using lean-burn strategies. Accordingly, lean mixtures can also afford higher compression ratios than stoichiometric mixtures, and this can further improve the theoretical engine efficiency, as shown in the equation above.

As far as pollutants are concerned, hydrogen combustion engines only produce trace amounts of carbon dioxide, carbon monoxide and hydrocarbon emissions. Due to the lack of carbon in the fuel, these small traces have been attributed to lube oil combustion [9]. However, oxides of nitrogen (NO_X) emissions are a result of high in-cylinder temperatures and can occur in hydrogen engines. Figure 3 shows a typical NO_X emissions trend of a hydrogen engine as a function of relative air/fuel ratio. Due to reduced combustion temperatures, lean homogeneous hydrogen-air mixtures in excess of λ=2 burn without forming NO_X emissions. However, engine operation at relative air/fuel ratios of $1<\lambda<2$ can result in high NO_X emissions levels that can exceed those of conventional gasoline engines. A typical NO_X emissions curve for homogeneous hydrogen combustion peaks around λ=1.3 and decreases when approaching stoichiometric conditions due to reduced oxygen availability.

Definition of state-of-the-art and advanced technology hydrogen engines

In the following sections hydrogen engines are categorized either as state-of-the-art or advanced technology. While the number of hydrogen vehicles and engines in the field is negligible compared to conventionally fueled engines, the term state-of-the-art is used nonetheless to define engine technology that has been demonstrated in prototype fleets. On the other hand, mixture formation concepts that have so far been limited to research engines or to single prototype vehicles are considered advanced technology. A differentiation of hydrogen mixture formation concepts can be done by (1) location of mixture formation equipment and (2) temperature of the introduced hydrogen. Injection or carburetion in the intake manifold or intake pipe of ambient temperature hydrogen has been widely used for demonstration vehicles and is therefore considered state-of-the-art technology. As shown in Figure 4, this mixture formation concept is very similar to conventional gasoline engine technology while both injection of cryogenic (very low temperature) hydrogen into the intake system and direct injection of hydrogen into the combustion chamber are considered advanced technologies. These three hydrogen mixture formation concepts differ in terms of engine performance and emissions behavior, current state of development and dissemination, and complexity and are further discussed in the following sections.

State-of-the-art hydrogen engine technology

Mixture formation

Because of its physical and chemical properties, hydrogen is mostly used in spark-ignited engines. Therefore, a conventional gasoline engine is used as baseline. In a gasoline engine, fuel is injected in the intake manifold, where it evaporates and mixes with air to form a homogeneous mixture by the time it is compressed in the cylinder. The injection of the fuel in the intake manifold is indicated by the term PFI (port fuel injection).

Figure 4 compares the theoretical maximum power output from a PFI gasoline and hydrogen engine per unit of engine displacement. The achievable power output of a hydrogen engine

is reduced compared to that of its gasoline counterpart due to the low volumetric density of hydrogen. Hydrogen occupies a larger amount of the available space in the engine which reduces the amount of air that can be aspirated into the cylinder. This negative effect is partially compensated by the higher heating value (more released energy per unit of mass) and stoichiometric air/fuel ratio (less fuel needed per unit of air), but it still theoretically results in a 17% lower achievable power output. Despite the lower theoretical power output compared to other mixture formation systems, PFI is the only mixture formation system used in demonstration vehicles because of its relative simplicity and availability of injection equipment.

Load control strategy

In a conventional gasoline engine, a throttle valve is used in the intake manifold to reduce the power output for part-load operation. Varying the throttle position controls the amount of mixture (air+fuel) inside the engine, while the air/fuel ratio is kept constant. Since the quantity of the mixture is controlled, it is also referred to as ‘quantitative’ load control strategy. Using a throttle valve results in poor part-load efficiency, because the partially closed valve represents a resistance for the flow (pumping losses) which requires work from the engine.

The wide flammability limits of hydrogen are an advantage for the load control strategy, since they allow a ‘qualitative’ load control strategy which avoids throttling in the intake manifold and the corresponding pumping losses. Here, the air/fuel ratio is increased to reduce the power output for part-load operation like in a diesel engine. Operating the engine with ultra-lean mixtures also has the advantage of reducing the engine-out NO_X emissions as shown in Figure 3.

Recirculation of exhaust gases back to the intake of the engine is another way to reduce the power output for part-load operation without throttling. The presence of the inert exhaust gases also reduces the amount of air and fuel inside the engine. Hydrogen allows stable engine operation with higher amounts of EGR (exhaust gas recirculation) compared to

gasoline because of the wider flammability limits and faster flame propagation.

The maximum achievable power output per unit of engine displacement can be increased by increasing the pressure in the intake manifold of the engine. Figure 5 demonstrates that the same power output of the reference gasoline engine can be achieved with hydrogen if the intake pressure is boosted by 1 bar and a relative air/fuel ratio of around 2 is used. The compressor that boosts the intake pressure can be driven mechanically (supercharging) or by a turbine that recovers the remaining energy in the exhaust gases (turbocharging). From an efficiency stand-point, turbocharging is considered the preferred option. However, reduced throttle response and reduced exhaust energy with hydrogen compared to conventional fuel operation make the implementation of a turbocharged hydrogen engine more challenging.

Applying one of the load control strategies mentioned above leads to a compromise either in terms of power density (for qualitative, lean-burn, approach) or engine efficiency (for quantitative, stoichiometric, approach). A potential solution to this trade-off is combining lean-burn and stoichiometric operating strategies [12,13,14]. At low engine loads, the engine is operated at variable lean air/fuel ratios, resulting in good engine efficiencies and extremely low engine-out emissions. Once a certain engine power demand is exceeded, the operating strategy is switched to throttled stoichiometric operation. The NO_X emissions critical operating regime at relative air/fuel ratios of $1<\lambda<2$ is avoided and a conventional after-treatment system can be used to reduce NO_X emissions in stoichiometric operation.

The engine performance provided by the load control strategy mentioned above is shown in the map in Figure 6, as a result of intensive research carried out on a single-cylinder engine at BMW [16]. This result was later scaled to the 12 cylinders case, for implementation in a demonstration vehicle. The map is characterized by an island of peak performance between 4 and 6 bar IMEP (indicated mean effective pressure) with an ITE (indicated thermal efficiency) of 42%. This peak efficiency along with much of the map showing ITE values

greater than 38% demonstrates promising engine performance using state-of-the-art engine technology. Unfortunately, it can also be seen in Figure 6 that the peak torque is approximately 10.3 bar IMEP meaning the power density is low relative to comparable gasoline engines. This load limit is largely the result of low intake charge density and partly the result of combustion limitations associated with abnormal combustion.

Abnormal combustion

The wide flammability limits and high flame speeds, combined with low required ignition energy, are beneficial for the efficiency of hydrogen engines, as explained above. However, these properties can also result in undesirable combustion phenomena. Much of the early work on hydrogen engines was targeted at trying to avoid these phenomena.

The most frequently cited phenomenon is called ‘backfire’, which is the early ignition of the hydrogen-air mixture during the intake stroke. This results in a combustion event in the intake, which could be damaged as a consequence. To avoid this premature ignition, care must be taken to prevent unwanted ignition sources such as hot spark plug electrodes, exhaust valves, etc., which implies some hardware modifications to the engine. Avoiding the presence of ignitable mixtures when there might be an ignition source, is another means to prevent backfire. Here, variable valve timing and carefully controlled injection timing have been used to avoid backfire occurrence by allowing a cooling phase with fresh air while limiting the presence of hydrogen during the early intake phase [17,18].

Unwanted ignition before the spark plug is fired can also occur when the intake valves are already closed. This undesired phenomenon is called ‘pre-ignition’. As the valves are closed and the cylinder charge is being compressed, this can lead to very high pressures and severe damage.

Finally, auto-ignition of the unburned mixture (knock) can occur like in any spark ignition engine. As explained in the introduction, compared to conventional gasoline engines, knock is less likely to occur in a hydrogen engine. However, the effect could be more severe,

because of the high burning velocity of hydrogen mixtures.

Demonstration vehicles

Port fuel injection of hydrogen is the state-of-the-art technology, already being implemented in several demonstration vehicles. The first category of vehicles includes those that have been converted from existing vehicles. The second category is for dedicated vehicles that have been fully developed for hydrogen operation.

The changes that have to be made to an existing vehicle in order to convert it to operate on hydrogen are limited to the fuel system (from storage to injection) and the engine control unit programming. Quantum Tecstar has converted over 30 vehicles to hydrogen operation using the Toyota Prius hybrid as a platform (Figure 7). Two tanks with compressed hydrogen replace the conventional gasoline tank, leaving the interior of the vehicle unchanged. The converted Prius engine is turbocharged in order to increase the power output on hydrogen operation. With similar drivability to the gasoline version, the Quantum Hydrogen Prius has an estimated range of 100 to 130 km, while meeting Super Ultra Low Emissions Vehicle (SULEV II) emissions standards [19].

Developing a dedicated hydrogen vehicle requires a higher number of considerations concerning the hardware [20]. With approximately 100 units built, the BMW Hydrogen 7 (Figure 8) is likely the hydrogen vehicle with the highest number of vehicles produced. The vehicle is equipped with a bi-fuel system allowing for operation on hydrogen or gasoline. On hydrogen, the car employs the combination of a variable air/fuel ratio lean-burn strategy at low and medium loads and a throttled stoichiometric strategy at high engine loads, which was described above. Approximately 8 kg of hydrogen are stored on the vehicle in a cryogenic tank that is located in the trunk which allows a range of 200 km on hydrogen. Emissions tests of a dedicated mono-fuel version of the Hydrogen 7 vehicles showed the low emissions potential of hydrogen powered vehicles. With a dedicated after-treatment design featuring two catalysts (one for stoichiometric operation and one for reducing NO_X peaks that

occur when switching from lean to stoichiometric operation) the vehicle achieved drive-cycle NO_X emissions that were approximately 0.0008 g/mi, which is equal to 3.9% of the SULEV II limit [21].

Advanced technology hydrogen engines

Cryogenic port fuel injection

Cryogenic port fuel injection is similar to conventional port fuel injection in terms of location of the mixture formation equipment. However, rather than introducing hydrogen at ambient temperature, the fuel is supplied at low, cryogenic temperatures, typically available when hydrogen is stored in its liquid form at approximately 20 K. The low temperature of the introduced hydrogen leads to the reduction of the temperature of the intake air when mixing and ultimately leads to increased charge density. While conventional hydrogen port fuel injection suffers from reduced power density compared to gasoline, hydrogen engine operation with cryogenic injection theoretically exceeds the power density of a comparable gasoline engine under stoichiometric conditions, as shown in Figure 4.

The performance benefits associated with cryogenic port injection include not only higher power density but also improved efficiency. The indicated thermal efficiency map in Figure 9 is taken from the same single-cylinder research engine at BMW as the PFI map in Figure 6. With the use of cryogenic PFI, the peak torque is increased by 25% to approximately 12.8 bar IMEP at the same engine speed [16]. Furthermore, greater charge density while using a qualitative load control strategy results in proportionally higher IMEP throughout the engine operating range. This effectively expands the 42% ITE operating range because air/fuel ratio is a key factor impacting efficiency in this engine [16]. Another benefit of using cryogenic PFI is improved knock resistance which allows spark timing to be optimized where it was previously limited by knock, namely during high load operation [16]. Improved spark timing results in higher ITE along the full load line at the top of the map in Figure 9.

While the increased power density as well as the improved engine efficiency make cryogenic port fuel injection a promising concept, there are still several remaining challenges. Application of cryogenic injection is only sensible in combination with liquid hydrogen on-board storage, a concept that has been proven to be feasible; however, cost and complexity of liquid on-board storage are significantly higher than compressed storage. Furthermore, injector performance and durability under cryogenic conditions needs to be investigated. Finally, introduction of cryogenic hydrogen into the intake manifold can lead to freezing of humidity contained in the intake air and can ultimately cause ice build-up around the injector.

Direct injection

As shown in Figure 4, a promising approach to increase the engine performance consists in injecting the fuel directly into the combustion chamber during the compression stroke, when the intake valves are closed. In the particular case of a fuel like hydrogen, the direct injection (DI) approach allows overcoming the loss of volumetric efficiency due to the gas phase fuel displacing air in the intake manifold. Accordingly, hydrogen DI engines can provide the same or higher power density than conventional gasoline engines. In order to perform the fuel injection during the compression stroke, the fuel injection pressure has to be higher than in the case of port fuel injection. To accomplish injection at late crank angles (against the high in-cylinder pressure) and to ensure the highest mass flow rate (occurring under sonic conditions), hydrogen DI injectors typically operate between 25 and 200 bar. Higher injection pressure leads to higher mass flow rate, however in a real vehicle this would potentially also reduce the range, since the hydrogen pressure in the tank would progressively decrease. Typically, an injection pressure of 100 bar represents a good compromise. Due to the high pressure, DI injectors require advanced and robust technology. Injectors are usually classified based on the actuator technology. The actuator commands the motion of the needle, thus regulating the fuel flow through the injector nozzle. In Figure 10, three injector generations (Electro-hydraulic injectors (EHI) – Electromagnetic valve (EMV) injectors – Piezo injectors) used in DI engines are shown. The main differences in the working principle

of the three injectors can be summarized as follows:

- EHI Injector. Uses an actuator (usually a solenoid) and a hydraulic oil servo system to lift the needle and inject the fuel. The needle valve is closed again through the hydraulic oil servo system (ON/OFF control).
- EMV Injector. Uses a solenoid actuator and a collapsing magnetic field to lift the needle and inject the fuel. The needle valve is closed by a spring (ON/OFF control).
- Piezo Injector. Uses a piezo-electric actuator to directly convert a voltage signal into needle lift. The lift is proportional to the applied voltage (analogue control).

The electro-hydraulic injector shown here was developed at Tokyo City University [22], while the solenoid (EMV) and piezo injectors were manufactured by Westport [23,24] and extensively tested at Argonne National Laboratory. The piezo-electric element represents the latest generation of injector actuators and ensures higher performance, in particular faster response, than the solenoid actuator because there is no need to generate a collapsing magnetic field. Accordingly, the piezo injector is capable of delivering higher average fuel mass flow than a solenoid injector.

Table 2 shows the main characteristics of the three examined injectors. Despite the lowest maximum needle lift and lowest rate of needle lift during the injector opening, piezo-injectors show the highest average mass flux, generally due to lower injection delay and faster fuel flow transient than EMV and EHI injectors. The EHI injector shows the highest maximum lift and flow area, however the extremely slow transients (due to the inertia of the hydraulic servo-system) condemn it to be characterized by the lowest performance in terms of fuel mass delivered in a certain amount of time.

The EMV injector is characterized by fast needle lift but the response is overall still slow due to the initial delay. Therefore, it is clear that a piezo-injector allows injecting a certain amount of fuel in much shorter time than a solenoid injector, for the same injection pressure. Moreover, piezo-injectors can manage higher injection pressure (up to 250 bar) than EMV

injectors.

The piezo-actuator technology significantly improved the durability of high pressure gaseous injectors. Nonetheless development of hydrogen injectors is particularly challenging due to a variety of factors including:

- The low density of hydrogen significantly reduces the internal damping effect which helps reducing the needle oscillation, especially during the transients (opening and closing).
- The low viscosity of hydrogen reduces the hydrodynamic lift effect, which helps to keep the injector internal parts separated and prevent shear stresses.
- Hydrogen is usually delivered as totally free of lubricant traces and is much drier than natural gas, thus relative motion between the sealing elements is detrimental to hydrogen injectors.
- Hydrogen potentially degrades epoxy resins used to coat the piezo stack

As a result, compared to liquid fuels or compressed natural gas (CNG), extreme precision has to be ensured for the opening and closing operations. The piezo injector offers several benefits in terms of needle lift control. Piezoelectric material is characterized by a well-known relationship between voltage and expansion, thus the lift control is much more precise than in solenoid injectors. This not only ensures excellent repeatability, but it allows modifying the waveform to provide the desired lift profile, depending on the engine operating condition. The lift and acceleration profile can be optimized to improve the needle seating, reduce the seat impact, control the needle bouncing, thus improving the injector durability.

The current generation of piezo injectors offers higher injection pressure and higher mass flow along with better repeatability and durability than the previous EHI or EMV injectors. It is also suitable for multiple injections, due to the fast response and high precision.
Nonetheless, research is still required to face remaining challenges concerning durability, control, size and cost. In particular, hydrogen may cause embrittlement of the injector

materials and can chemically attack the oxide layer of the metallic surfaces, thus leading to fracture and wear respectively. Research in the proper coatings and materials as well as in reducing friction and impact wear can improve the injector durability.

In some cases, modified versions of the solenoid injector (dual solenoid [25]) can achieve almost the same performance of piezo injectors, but with half the size and much lower cost. Therefore, depending on the scope (research or series production), on the required performance (mass flow rate, number of injections) and on cost and size constraints, the old generation solenoid injectors may still be more desirable than new generation piezo-actuated injectors. The latter technology has yet to overcome limiting issues concerning high production costs and large size of the piezo-stack.

Independently on the injector technology, DI offers higher flexibility than PFI in defining the proper strategy to achieve high thermal efficiency. This also means higher number of degrees of freedom since injection timing, number of injections, injector location, and nozzle geometry, significantly influence the final stratification of the charge around the spark-plug at the time of spark ignition. Figure 11 shows the basic strategies for direct injection, defined on a time-scale where the ignition timing is represented by the spark symbol. High load conditions require a large amount of hydrogen injected. Accordingly, in a single-injection approach, the injection cannot be started too close to the TDC (Top Dead Center), since the end of injection (EOI) has to occur before the spark timing. To increase stratification around the spark-plug at the ignition timing, a multiple injection strategy can be adopted, where hydrogen is injected immediately before and during the combustion event.

In general, the main goals and challenges in a direct injection strategy can be defined as follows:

1. Perform late injection: Late injection allows increasing the thermal efficiency due to decreased compression work. It also allows providing highly stratified mixtures, since there is not enough time for complete mixing of the fuel with air.

2. Properly stratify the mixture at the spark-timing (see Figure 12): The ideal mixture stratification consists of a stoichiometric or rich mixture around the spark-plug at spark timing and an ultra-lean mixture close to the cylinder walls. The engine efficiency benefits from such a configuration due to increased combustion efficiency and reduced losses from heat transfer to the cylinder walls.

Pollutant emissions are influenced by the mixture stratification as well. Figure 1 shows that hydrogen can still be burned efficiently in ultra-lean mixtures (λ>2) and Figure 3 shows that in these lean conditions the NO_X emissions are extremely low. At the same time, when mixtures are highly stratified, richer zones may exist thus increasing NO_X emissions even if the mixture is lean overall.

It becomes evident that the injection timing (start of injection, SOI) is not the only parameter to be controlled in order to optimize performance and emissions in a direct injection hydrogen engine. In order to pursue the ideal mixture stratification shown in Figure 12, nozzle geometry, injector location, piston shape and combustion chamber design become very important parameters. At Argonne National Laboratory, computational fluid dynamics (CFD) is being used to support engine testing. CFD numerical simulations provide deep insight into the mixture formation process and are used as an effective development tool, with the final goal of pursuing the ideal mixture stratification.

CFD results have been extensively validated against PIV (Particle Image Velocimetry) and PLIF (Planar Laser-Induced Fluorescence) data from an optically accessible engine [26,27] and have been subsequently used to optimize the injector nozzle geometry. As shown through the CFD results in Figure 13, even in the case of extremely simple chamber geometry (pent-roof with flat piston) the mixture stratification is significantly affected by the nozzle configuration.

Hydrogen jets not only interact with the cylinder walls and the existing flow field, but they may also interact with each other, due to the Coanda effect [28]. The number and diameter of

holes in the injector nozzle greatly influence the evolution of each jet. However, in order to maximize the mass flow rate, the total flow area cannot be larger than the critical area between the needle valve and its seat. Accordingly, the nozzle geometry is the main factor responsible for an efficient stratification at the time of ignition. Conversely, as far as the injection duration is concerned, the actual bottle neck is represented by the actuator characteristics (nominal injection pressure, needle response, maximum needle lift and flow area).

Realizing Ideal Mixture Stratification

Currently, research is taking place to realize ideal hydrogen mixture stratification in an internal combustion engine to demonstrate its potential for high efficiency and low emissions. Multiple engine concepts have been developed to realize ideal mixture stratification.

One recent example is the work of Heindl et al. [29] in which a diesel like engine concept was developed to perform stratified, diffusive combustion of hydrogen jets in a ω-shaped piston bowl. One focus of the work was to locate the injector nozzles and design the piston bowl such that the hydrogen jets would have the maximum possible time for combustion before impinging the combustion chamber walls. The idea is to ignite the injected hydrogen immediately upon entering the combustion chamber to prevent combustion from taking place in close proximity to the combustion chamber walls. This concept requires a very high injection pressure in order to overcome the in-cylinder pressure near TDC, especially when the mixture is combusting during injection and at higher engine loads where more fuel is required.

A key consideration in order to effectively perform stratified, diffusive combustion is ignition timing. Heindl et. al. explored various ignition methods including a pilot injection to facilitate ignition of a homogeneous mixture by which the main injection would be ignited. Compression ignition of the homogeneous charge was possible with the use of intake air heating but more stable combustion resulted from using a spark plug to ignite the

homogeneous mixture. An indicated thermal efficiency based only on the high pressure part of the cycle (ITE_hp) of 44% was achieved [29]. It is worth noting that ITE_hp overestimates the ITE, which is otherwise calculated based on the entire cycle. Comparable efficiency and combustion stability were also demonstrated using a glow plug mounted close to the injector in order to directly ignite the hydrogen jets. In this case a pilot injection was not possible because it would be subject to uncontrolled ignition by the glow plug so the entire charge was subject to stratified, diffusive combustion and ignition timing was dependent on injection timing.

A similar engine concept using a diesel-like combustion chamber but with a spark plug mounted near the injector nozzle has been studied by Tanno et al. [30]. The engine concept used a hydraulically actuated injector which was centrally located in the combustion chamber in order to aim multiple hydrogen jets into a ω-shaped piston bowl. This study highlighted the importance of jet penetration because the location of the stratified mixture at ignition timing depends on how quickly the jets travel through the combustion chamber. Jet penetration is dictated by injector nozzle design and injection pressure (in this case the injector is rated to 300 bar). Using injection pressure to control mixture stratification, an injection pressure of 100 bar allowed the engine to operate with a peak ITE of 52% at 2000 rpm, 2.5 bar IMEP [30]. Using 100 bar injection pressure limited the amount of fuel that could be delivered because injection was taking place near TDC thus the engine was limited to low load in this case. Injection pressure was increased at medium to high loads to the detriment of ideal mixture stratification resulting in an ITE of 43.8% at 2000 rpm, 8 bar IMEP [30]. EGR was used to mitigate NO_X at this operating point and the resulting NO_X emissions were 0.35 g/kWh for this condition [30]. Future work on this diesel-like engine concept is intended to expand the operating range while managing jet penetration for improved efficiency, possibly through a different nozzle design, and continued use of EGR to mitigate NO_X.

Research at Argonne National Laboratory focused on the development of a partially stratified combustion system based on a typical SI combustion chamber design. Using a pent roof

head and flat piston top, the mixture formation process is controlled using injector nozzle geometry coupled with injection timing. The engine configuration is shown in Figure 12 with a centrally located injector nozzle and a spark plug mounted near the nozzle. An example of the mixture formation process is depicted in Figure 13, which shows that injector nozzle geometry is critical to achieving ideal mixture stratification. Recent developments, based on collaborative engine testing and multi-dimensional CFD engine modeling, have led to a 4-hole injector nozzle operated at SOI times from 60 to 120 °CA BTDC at engine speeds from 1000 to 3000 rpm respectively. SOI can be delayed as engine speed decreases while still allowing sufficient time for mixture formation. SOI was optimized as a function of engine speed based on a series of SOI sweeps at different operating speeds. The resulting SOI trend is a 15 °CA delay per 500 rpm decrease in engine speed.

The results for engine performance shown in Figure 14 and Figure 15 are presented in terms of brake engine values. This requires a friction assumption since the single-cylinder research engine is understood to have inherently greater friction than a multi-cylinder counterpart. Since the engine geometry (89 mm bore and 105.8 mm stroke) is representative of a light-duty automotive engine, friction values from a similar multi-cylinder engine have been applied to the measured single-cylinder results [31]. Brake engine values as shown in subsequent engine maps are based on the estimated work output from the engine through the crankshaft to the rest of the powertrain.

The partially stratified concept provides promising results not only for peak efficiency but also over an operating range which is relevant for vehicle applications. The engine operates above 35% BTE over approximately 80% of the tested operating range from 1000 to 3000 rpm and from 1.7 to 14.3 bar BMEP [31]. The peak efficiency point occurs at 2000 rpm and 13.5 bar BMEP with a BTE value of 45.5% as specified on the map in Figure 14 [31]. The other specified operating point with a BTE of 33.3% is 1500 rpm and 2.3 bar BMEP [31] which represents a typical part load operating point.

Compared to engine maps for PFI and cryogenic PFI mixture formation strategies (Figure 6 and Figure 9 respectively) the operating range for the DI engine is limited by 3000 rpm maximum speed but includes a broader range of engine loads. Within the comparable operating range, the partially stratified H_2-DI engine concept shows a substantial improvement in thermal efficiency (note that friction losses have been included in Figure 14 and not in the previous maps) and the peak efficiency is observed at higher load. The peak torque is also increased reaching a maximum of 14.3 bar BMEP. The preconceived benefit of DI to increase charge density (Figure 4) is only partially responsible for higher peak torque because simulated turbocharging was also used on the optimized DI engine.

A constant relative air/fuel ratio (λ=3.3) control strategy was employed whenever possible [31] over the tested operating range. This was done through variable injection duration for fuel metering and simulated turbocharging for air/fuel ratio control. To simulate turbocharging the exhaust back pressure was set as a function of intake pressure. This function was validated to ensure that simulated turbocharging was in-line with the capability of a real turbocharger [31]. The constant λ=3.3 strategy was chosen because it was found to be sufficiently rich to provide flame speeds conducive to ideal combustion phasing while sufficiently lean to mitigate NO_X formation. It is interesting to note that λ may be further optimized especially in conjunction with different injector nozzle designs and mixture formation concepts. The aforementioned benefits of using λ=3.3 were determined experimentally for the given engine configuration.

An engine map of NO_X emissions corresponding to the efficiency map in Figure 14 is shown in Figure 15. Results show that the partially stratified mixture formation concept coupled with the overall lean control strategy provides relatively low NO_X emissions. Although no aftertreatment is used, the map is dominated by NO_X emissions less than 0.10 g/kWh with lower NO_X emissions observed at lower engine load. Despite a peak NO_X of 1.55 g/kWh at 3000 rpm and high load, lower engine loads are more relevant to engine operation in vehicular applications. The map of engine out emissions therefore provides promising results

for evaluation of hydrogen vehicle emissions which is discussed in a later section.

Assessment of present challenges and future potential

The previous sections have highlighted the enormous potential of hydrogen engines in achieving high thermal efficiency and low impact on the environment. Nevertheless, challenges still remain to be addressed in order to increase the efficiency even further. Heat transfer to the cylinder walls is the largest efficiency loss within the cylinder-piston thermodynamic system. In a PFI strategy, this loss is mainly a function of the fuel properties and of the air/fuel ratio. With a DI strategy, it also depends on the stratification of the charge. This section first investigates the heat transfer to the walls in detail for state-of-the-art (PFI) and advanced (DI) technologies. Then, other contributions to the total efficiency loss are discussed for the advanced (DI) technology. Finally, the potential application of the advanced technology to a real light-duty vehicle is evaluated by means of a simulation tool and the estimate of performance in terms of fuel consumption and emissions is provided.

Analysis of heat transfer in hydrogen engines

The investigation of the heat transfer inside internal combustion engines has always been a topic of interest in the search for higher power output, higher engine efficiency and lower emissions. However, only a few research groups have investigated it in hydrogen engines, because measuring the instantaneous heat loss during the combustion cycle is challenging.

Extensive research has been performed by teams working at Graz University of Technology and BMW. They focused on the investigation of combustion concepts for hydrogen engines. Heat transfer measurements were an important part of the research program to examine the effect of the heat loss on thermal efficiency. Wimmer et al. [32] compared the heat loss of hydrogen and gasoline combustion and concluded that the peak and total cycle heat transfer was higher for hydrogen. They investigated both injection strategies discussed above (PFI and DI). Both peak and total cycle heat losses were higher for DI than for PFI, because the injection process during the compression stroke augments the in-cylinder turbulence and

consequently the heat transfer. Eichlseder et al. [33] however showed lower total cycle heat losses with stratified direct injection concepts. Both studies showed that the heat loss is an important factor for efficiency optimization in hydrogen engines. Michl et al. [34] measured heat flux on the cylinder head and piston at a total of 29 positions. They concluded that the air/fuel ratio and the amount of exhaust gas recirculation (EGR) have a large influence on the heat loss. It would be beneficial to operate the engine on lean mixtures or with high amounts of EGR to reduce the heat loss. Shudo et al. [35,36,37] have also done research on the heat loss in hydrogen engines to increase the thermal efficiency, first with PFI and later with DI. They investigated the influence of ignition timing and air/fuel ratio and compared hydrogen to methane combustion, concluding that hydrogen combustion results in higher heat losses. However, the engine loads of the operating points were not published, so it is not clear whether the measurements on both fuels resulted in similar engine loads. The thermal efficiency increased with increasing the relative air/fuel ratio λ because of lower heat losses, confirming the results of Michl et al. [34]. Based on measurements in a constant volume chamber, Shudo et al. [36] found stratified direct injection to be the best strategy to increase the thermal efficiency of hydrogen engines, which agrees with the conclusions of Eichlseder et al. [33]. Wei et al. [38] investigated the heat transfer in a hydrogen engine with dual injection (PFI at low loads and DI at high loads), comparing it to gasoline. The peak of the heat flux was 2.5 times larger for hydrogen under the same engine speed and load.

Based on the literature described above, it could be concluded that the heat loss of hydrogen is always higher than that of any other fuel. However, the comparisons were not done in a wide range of similar engine loads. Therefore, this section compares the heat loss in a PFI engine operated on hydrogen and methane in a range of similar indicated power outputs at a constant speed of 600 rpm. A detailed description of the measurement setup and method can be found in [39]. The power output for hydrogen was controlled by varying the relative air/fuel ratio. In contrast, a throttle was used in the intake manifold for methane (λ=1). The ignition was always at MBT-timing.

Three different relative air/fuel ratios were selected for hydrogen (λ = 2, 1.5 and 1), which resulted in an indicated work output (Wi) of 287, 327 and 376 J, respectively. The corresponding engine IMEP's (indicated mean effective pressure) were 4.7, 5.3 and 6.1 bar. The comparable three indicated power outputs on methane were 294 J (Throttle Position, TP, at 77°), 317 J (TP at 76°) and 367 J (TP at 74°). The heat flux measurements at a certain position on the cylinder liner are plotted in Figure 16, those of hydrogen with a solid line and those of methane with a dotted line. The lowest, middle and highest engine load are in black, red and blue, respectively.

The initial increase in the heat flux traces is caused by the flame passage over the measurement position. Although the flame speed is slower for the leanest hydrogen measurements (black color), the initial rise occurs at the same instant of the stoichiometric measurement (blue color) due to the advanced ignition timing.

For hydrogen, the fast and short combustion of the stoichiometric measurement generates a high peak in the heat flux trace. This peak greatly reduces if the engine is operated on a lean mixture. The peak in the heat flux trace is reduced by 80% when λ is changed from 1 to 2. The resulting power output decreases by 23%. In contrast, the heat flux traces of methane remain almost identical. Reducing the in-cylinder mass has a large effect on the resulting power output, but not on the heat loss. The heat transfer does decrease when the load is reduced, but not as much as expected. The air/fuel ratio on the other hand has a great influence on the heat transfer process. The peak in the stoichiometric heat flux trace of hydrogen is 3 times higher compared to methane, but it is smaller if λ is equal to two.

The difference in the heat transfer process is reflected in the indicated efficiency of the engine. To demonstrate this, an estimate of the total cycle heat loss is calculated assuming that the heat flux at the measurement position represents the heat flux over the entire cylinder wall. The most important data of the measurements are summarized in Table 3. For hydrogen, the total cycle heat loss decreases from 597 J to 235 J if the power output is

reduced from 367 J to 294 J, which is a reduction by 61%. The heat loss through the cylinder walls for methane reduces from 386 J to 343 J which is only a reduction by 11%.

For the highest power output, the indicated efficiency for hydrogen is lower (23%) compared to that for methane (26%) due to the higher heat loss. The indicated efficiencies for both fuels are almost the same for the middle power output and that of hydrogen becomes higher at the lowest engine load, 29% compared to 25% for methane. Although there is a difference of 10% in the total cycle heat loss between hydrogen and methane at the highest engine load, there is only a difference of 3% in the indicated efficiency. The higher combustion efficiency caused by the fast combustion process of hydrogen partially counters the high amount of heat loss through the cylinder walls. The results of Shudo et al. [35] showed a similar trend. The difference in heat loss between hydrogen and methane was around 20%, whereas the difference in indicated efficiency was only around 5%.

The results presented here, combined with the findings in the literature, demonstrate that a hydrogen engine should be operated with a lean mixture to obtain high engine efficiency. Exhaust gas recirculation in combination with supercharging could be used to achieve high engine loads without increasing the high heat losses. A remaining challenge is the development of a heat transfer model for internal combustion engines which is capable of predicting the large variation in the heat loss for operation on hydrogen, since it has been shown that current models are not suitable [40,41].

Analysis of efficiency losses in a DI hydrogen engine

This section provides a comprehensive analysis and quantification of the efficiency loss contributions in a DI engine. The efficiency analysis begins with a theoretical maximum efficiency of the engine based on the engine geometry and properties of the air-fuel mixture. This efficiency of an ideal engine with real charge is termed η_{IRC} and is labeled on the y-axis in Figure 17. Consider, for example, a compression ratio of 12:1 and a relative air/fuel ratio of λ=2 on the plot in Figure 17, η_{IRC} is approximately 55% meaning the greatest achievable

engine efficiency will always be less than that value. From this plot it could be concluded that continually increasing compression ratio will result in continually increasing engine efficiency; however, this is not the case because many partial losses also increase with compression ratio resulting in a tradeoff between η_{IRC} and partial losses with respect to compression ratio.

The difference between air aspirating and mixture aspirating operation takes into account the added work required to compress hydrogen during the compression stroke. For PFI operation η_{IRC} is based on mixture aspirating operation because hydrogen is present during the entire compression stroke while in DI engines hydrogen is added during the compression stroke. The ideal cycle for DI operation would therefore be an instantaneous addition of hydrogen at TDC. The equation and terminology used for the analysis of losses are as follows [42]:

$$BTE = \eta_{IRC} - \Delta ICS - \Delta IC - \Delta RC - \Delta WH - \Delta GE - \Delta F$$

BTE	brake thermal efficiency
η_{IRC}	efficiency of ideal engine with real charge
ΔICS	losses due to injection during
ΔIC	losses due to incomplete combustion
ΔRC	losses due to real combustion
ΔWH	losses due to wall heat
ΔGE	gas exchange losses
ΔF	friction losses (multi-cylinder counterpart)

ΔICS is specific to DI engines and accounts for the fact that the real injection process is not an instantaneous addition of hydrogen at TDC. Rather it is an addition of hydrogen of finite duration with an SOI time that has to allow the proper amount of time for ideal mixture stratification. ΔICS monotonically decreases with delayed SOI but in the case of the partially stratified engine concept SOI time is optimized between 60 and 120 °CA BTDC depending on engine speed. This results in an efficiency loss of nearly 1.6% (Figure 18).

ΔIC accounts for hydrogen that escapes combustion typically by being compressed into the crevice volume or flame quenching zone of the combustion chamber. ΔIC is a small loss under normal conditions unless the mixture formation process leaves substantial quantities of hydrogen in the crevice or quenching zones.

Losses due to real combustion, ΔRC, account for the real heat release profile in the engine. While η_{IRC} assumes constant volume combustion at TDC, real combustion requires a finite period of time with the majority of heat release taking place after TDC. The fast laminar flame speed of hydrogen mixtures, albeit a function of local air/fuel ratio, provides relatively short combustion durations which serve to minimize ΔRC. Moreover, proper mixture stratification around the spark plug reduces the ignition delay and allows combustion phasing to be optimized which also serves to minimize ΔRC. From the evaluation of ΔRC in the partially stratified H_2-DI engine it can be seen that this is a significant efficiency loss. These results along with the other partial losses are shown in Figure 18. ΔRC equates to a 2.7% and 3.2% loss in efficiency at the low and high load operating conditions respectively.

Efficiency losses due to wall heat, ΔWH, are 9.1% and 4.6% which for both operating conditions is the most significant loss mechanism. The general trend in ΔWH, is that it increases at lower engine speeds because there is more time per cycle for the combustion gases to interact with the combustion chamber walls. A tradeoff exists between ΔWH increasing with lower engine speed and other partial losses which tend to decrease and this tradeoff results in the peak efficiency being observed at 2000 rpm (Figure 14) [31]. In terms of engine load, one would expect ΔWH to increase with increasing load because the in-cylinder temperatures are higher. However, the trend is reversed when ΔWH is considered as a percentage of the total heat release as it is in Figure 18. The 1500 rpm low load operating condition exhibits almost twice the efficiency losses due to wall heat compared to 2000 rpm high load. This is because the heat losses increase with the load but the total heat release increases as well.

In the previous section the typical trend was an increase of ΔWH with increasing engine load even when calculated as a percentage of efficiency loss. At the same time, the effect of heat transfer losses on the indicated efficiency is a complex function of engine speed, load, and load regulating strategy. As an example, in Table 3 the hydrogen engine load is regulated by the relative air/fuel ratio λ ranging from 1 (high load) to 2 (low load). Accordingly, the cylinder

temperature during combustion at high load is expected to be higher than for the low load and this increases the heat transfer to the walls.

A further reduction in ΔWH is possible with a DI strategy. As discussed earlier in the Direct Injection section, the optimal stratification of the mixture within the cylinder has been the main goal of collaborative experimental and numerical efforts. With ideal mixture stratification (Figure 12), it would be possible to simultaneously reduce the heat transfer (ΔWH) and real combustion (ΔRC) losses. Furthermore, as discussed in the same section, achieving ideal stratification with late injection would also reduce the compression losses (ΔICS). Therefore a DI strategy not only provides higher performance but also offers higher potential in further improving such performance, due to the high flexibility in optimizing the mixture preparation process.

Gas exchange losses, ΔGE, are the result of pumping work that is required to exhaust spent gases and intake a fresh charge. The amount of pumping work required largely depends on the load control strategy being employed and whether it requires throttling or not. The wide flammability limits of hydrogen generally allow less throttling providing an inherent efficiency benefit. In the case of the partially stratified H_2-DI engine with the prescribed λ=3.3 control strategy, throttling was only required for loads less than 4 bar BMEP. The effect of throttling can be seen in Figure 18 where ΔGE is a 4.2% loss at low load and a negligible loss at high load. The high load operating point was run using simulated turbocharging with a 1.0 bar boost (2.0 bar absolute) and 0.2 bar differential pressure between the intake and exhaust manifolds.

The final loss mechanism being considered is friction, ΔF, and it is important to note that the friction values are taken from a multi-cylinder engine that is similar in geometry to the single-cylinder research engine. Similar to ΔWH, the trend in efficiency loss in terms of percentage is counterintuitive because friction is expected to increase with both engine speed and load. The expected trend is true in terms of absolute energy loss but ΔF still makes up a lesser

percentage of the total heat release at the high load operating condition in Figure 18.

Evaluating performance and emissions of DI hydrogen vehicles

Thus far only state-of-the-art hydrogen engines have been evaluated by their intended use in light-duty vehicles and advanced hydrogen engines by definition have not yet been implemented in vehicles for on-road testing. Vehicle simulations are used in lieu of experimental data in order to evaluate the future potential of advanced hydrogen engines. Having shown efficiency and emissions maps as well as an efficiency analysis (Figure 14, Figure 15, and Figure 18 respectively) from the partially stratified H_2-DI engine concept, this example will be carried forward for the subsequent vehicle simulation results.

Vehicle simulations are carried out using the Autonomie vehicle simulation tool [43]. The hydrogen engine under consideration is intended for light-duty automotive applications so the simulated vehicle is a midsize sedan with a 5-speed automatic transmission. The vehicle mass is 1553 kg, it has a footprint of 47.6 ft^2 (the footprint in ft^2 is used for calculating CAFE fuel economy), and it has a conventional (non-hybrid) powertrain [44]. The engine parameters were scaled to 2.0, 2.5, and 3.0 L displacement based on results from the 0.68 L research engine. City fuel economy is based on the UDDS driving cycle, highway fuel economy is based on the HWFET driving cycle, and combined fuel economy is based on a weighted average (55% city and 45% highway). These are evaluated in miles per gallon (mpg) of gasoline based on equivalent energy consumption.

Vehicle simulation results are presented in Figure 19 in the context of yearly CAFE fuel economy standards and U.S. EPA NO_X emissions categories. CAFE fuel economy standards are based on the vehicle footprint and it is important to note that unadjusted EPA values are used to provide a meaningful comparison to CAFE standards. Likewise, CAFE credits for alternative fuels are not considered in calculating the fuel economy. It follows from the promising engine efficiency values that the vehicle fuel economy exceeds 2016 CAFE standards even with a larger engine. The effect of engine downsizing is improved fuel

economy because the engine is being pushed into its higher load operating regime where the peak efficiency is observed. Vehicle fuel economy increases from 38.9 to 45.4 mpg when the hydrogen engine is downsized from 3.0 to 2.0 L [44].

There is clearly a tradeoff between fuel economy and NO_X emission that comes with engine downsizing. As the engine is pushed into its higher efficiency operating regime this is also a higher NO_X operating regime. The 2.0 L hydrogen engine emits 0.028 g/mile of NO_X [44] which is well within the U.S. DOE emissions target of Tier II Bin 5 (0.07 g/mile [45]) for hydrogen powered vehicles [43]. With the larger 3.0 L engine the NO_X emissions are significantly less with a value of 0.017 g/mile which falls within the SULEV II category [44]. This estimate comes from engine-out emissions data meaning hydrogen engines have the potential to achieve SULEV II emissions levels without the need for any exhaust aftertreatment.

Conclusions

Hydrogen is a promising fuel for internal combustion engines. However, its physical and chemical properties pose significant challenges for the design of hydrogen engines and vehicles. In particular, low density (low storage and power density), low ignition energy (combustion anomalies), low quenching distance and high flame temperature (high efficiency losses for heat transfer to the cylinder walls), significantly affect hydrogen vehicles in terms of performance, range and safety. Nonetheless, the chemical structure of hydrogen and its wide flammability range allow efficient and clean combustion, since high compression ratio and ultra-lean mixtures can be used, the latter also reducing the only significant pollutant produced (NO_X) during the combustion of hydrogen.

Because of its properties, hydrogen is mostly used in spark-ignited engines. Compared to conventional gasoline spark-ignition engines, hydrogen engines are affected by the loss of volumetric efficiency. Even though hydrogen has a higher heating value than gasoline, port fuel injection (PFI) hydrogen engines are theoretically doomed to deliver 17% lower power

density than gasoline engines. Nevertheless, by combining lean-burn (low load) and stoichiometric (high load) strategies, peak indicated efficiency of 42% could be reached together with a peak IMEP of 10.3 bar. State-of-art (PFI) technology has already been implemented in several demonstration vehicle prototypes that can be classified in converted (e.g. Quantum Hydrogen Prius, 130 km maximum range and NO_X emissions meeting the SULEV II limits) and dedicated (e.g. BMW Hydrogen 7, 200 km range and NO_X emissions well below the SULEV II limits) vehicles.

Cryogenic PFI can be considered as one of the advanced hydrogen engine technologies. It has the potential to increase the power density (even higher than in conventional gasoline engines) through the injection of hydrogen at cryogenic temperatures, thus reducing the temperature of the intake air and increasing the volumetric efficiency. Cryogenic PFI has demonstrated to be able to provide higher peak torque (12.8 bar IMEP) and to expand the 42% indicated efficiency to a broader range of operating conditions compared to standard PFI.

Direct injection (DI) is another advanced hydrogen engine technology that aims at injecting hydrogen directly into the cylinder at elevated pressures (typically around 100 bar), after the intake valves close. Direct injection increases the power density of hydrogen engines to levels potentially higher than in conventional gasoline engines. Furthermore, it provides high flexibility for optimizing the mixture formation process, which significantly affects combustion. Today, the new generation of piezo-actuated injectors allows providing high injection pressure (up to 250bar), large fuel flow rate, fast response, remarkable repeatability, and precise control of the needle lift. The later also allows reducing the needle seating impact and bouncing, thus improving the durability with respect to the previous generations of solenoid-actuated injectors. The large flow rate delivered through a piezo-injector can help performing late injection, which leads to a benefit in terms of indicated thermal efficiency. Also, advanced research in injector geometries and mixture formation concepts can help realizing ideal mixture stratification, consisting of the stratification of hydrogen around the

spark plug and far from the cylinder walls.

With a dedicated injector nozzle and an optimized DI strategy, adjusting the injection timing on the basis of engine speed and load, a single-cylinder research DI hydrogen engine delivered 45.5% peak brake thermal efficiency (almost 48% indicated thermal efficiency) and a brake thermal efficiency higher than the peak value for gasoline engines over 80% of the tested operating range, from 1000 to 3000 rpm and from 1.7 to 14.3 bar BMEP. Compared to cryogenic PFI, the range of tested engine speed is narrower but the DI engine shows higher peak load (14.9 bar IMEP). Furthermore, most of the operating conditions were turbocharged with a relative air/fuel ratio λ of 3.3, which provided extremely low NO_X emissions.

Current performance and emissions from hydrogen engines are already at a very good level, especially if compared to those provided by conventional spark-ignition gasoline engines. Nonetheless, this chapter also focuses on the remaining challenges and provides an estimate of future potential of hydrogen engines in terms performance and emissions. A comprehensive analysis of the heat transfer in a hydrogen engine is mandatory because it is the largest efficiency loss for state-of-art and advanced technology engines at a majority of the tested operating conditions. In the particular case of hydrogen, it has been demonstrated that the relative air/fuel ratio λ plays a key role in the high heat flux measured on the cylinder walls, caused by the high temperature during combustion. Generally, lean hydrogen/air mixtures produce low heat transfer to the walls, and thus lower efficiency loss.

The analysis of the efficiency losses can be expanded in case of the DI strategy, since through the injection strategy is also possible to simultaneously reduce more than one contribution to the total efficiency loss. Future research on DI hydrogen engines should aim at performing late injection and pursuing the concept of ideal stratification. As a result, the efficiency losses due to compression work, real combustion, and heat transfer to the wall, can be reduced.

The vehicle simulation tool Autonomie was used in order to provide an estimate of

performance and emissions delivered by an advanced DI engine when applied to a real light-duty vehicle. Results show that with a 3.0L engine is possible to achieve a combined fuel economy of 38.9 mpg and NO_X emissions of 0.017 g/mile (below the SULEV II limit). If the engine is downsized to 2.0L, the vehicle fuel economy increases to 45.4 mpg. NO_X emissions increases as well, 0.028 g/mile, just above the SULEV II limit but well below the target set by the U.S. Department of Energy (Tier II Bin 5, 0.07 g/mile).

Even though the vehicle results are only predictions based on vehicle simulations, fuel economy and NO_X emissions estimates demonstrate the enormous potential of hydrogen as a fuel for internal combustion engines especially since it was estimated that the SULEV II limits can be met without the need for any after-treatment device.

Acknowledgement

Parts of the submitted manuscript have been created by UChicago Argonne, LLC, Operator of Argonne National Laboratory (‘‘Argonne’’). Argonne, a U.S. Department of Energy Office of Science laboratory, is operated under Contract No. DE-AC02-06CH11357. The U.S. Government retains for itself, and others acting on its behalf, a paid-up nonexclusive, irrevocable worldwide license in said article to reproduce, prepare derivative works, distribute copies to the public, and perform publicly and display publicly, by or on behalf of the Government.

Research referenced in this manuscript was partially funded by DOE’s FreedomCAR and Vehicle Technologies Program, Office of Energy Efficiency and Renewable Energy. R. Scarcelli, N. Matthias and T. Wallner wish to thank Gurpreet Singh and Lee Slezak, program managers at DOE, for their support.

References

[1] U.S. Department of Energy office of Energy Efficiency and Renewable Energy.

“FreedomCAR and Fuel Partnership Plan”. Retrieved 5/4/2011: http://www1.eere.energy.gov/vehiclesandfuels/pdfs/program/fc_fuel_partnership_plan.pdf

[2] D. Abbott "Keeping the energy debate clean: How do we supply the world's energy needs?", Proc. IEEE, vol. 98, no. 1, pp.42 - 66 , 2010.

[3] Bradley D, Hicks RA, Lawes M, Sheppard CGW, Woolley R. The measurement of laminar burning velocities and Markstein numbers for iso-octane–air and iso-octane–n-heptane–air mixtures at elevated temperatures and pressures in an explosion bomb. Combust Flame 1998;115:126–44.

[4] Gu XJ, Haq MZ, Lawes M, Woolley R. Laminar burning velocity and Markstein lengths of methane–air mixtures. Combust Flame 2000;121:41–58.

[5] Verhelst S. A study of the combustion in hydrogen-fuelled internal combustion engines. PhD thesis, Ghent University, 2005. http://hdl.handle.net/1854/3378.

[6] Knop V, Benkenida A, Jay S, Colin O. Modelling of combustion and nitrogen oxide formation in hydrogen-fuelled internal combustion engines within a 3D CFD code. Int J Hydrogen Energy 2008;33:5083–97.

[7] Heywood JB. Internal combustion engine fundamentals. McGraw-Hill; 1988.

[8] Verhelst S, Sierens R, Verstraeten S. A critical review of experimental research on hydrogen fueled SI engines. SAE Paper No. 2006-01-0430 (2006).

[9] Rottengruber H, Wiebicke U, Woschni G, Zeilinger K. Wasserstoff-Dieselmotor mit Direkteinspritzung, hoher Leistungsdichte und geringer Abgasemission. Teil 3: Versuche und Berechnungen am Motor. Motortechnische Zeitschrift 61 (1999).

[10] Wallner T, Nande A, Naber J. Evaluation of injector location and nozzle design in a direct-injection hydrogen research engine. SAE Paper No. 2008-01-1785 (2008).

[11] Tang X, Stockhausen W.F, Kabat D.M, Natkin R.J, Heffel J.W. Ford P2000 hydrogen

engine dynamometer development. SAE Paper No. 2002-01-0242.

[12] Eichlseder H, Wallner T, Freymann R, Ringler J. The potential of hydrogen internal combustion engines in a future mobility scenario. SAE Paper No. 2003-01-2267.

[13] Enke W, Gruber M, Hecht L, Staar B. Der bivalente V12-Motor des BMW Hydrogen 7. MTZ vol. 68, no. 6, pp. 446−453, June 2007.

[14] Rottengruber H, Berckmüller M, Elsässer G, Brehm N, Schwarz C. Operation strategies for hydrogen engines with high power density and high efficiency. 15th Annual U.S. Hydrogen Conference. 2004: Los Angeles, California.

[15] Verhelst S, Maesschalck P, Rombaut N, Sierens R. Efficiency comparison between hydrogen and gasoline, on a bi-fuel hydrogen/gasoline engine. International Journal of Hydrogen Energy, 2009. 34(5): p. 2504-2510.

[16] Verhelst, S.; Wallner, T.; Eichlseder, H.; Naganuma, K.; Gerbig, F.; Boyer, B.; Tanno, S: 'Electricity Powering Combustion: Hydrogen Engines.' Proceedings of the IEEE. Volume 100. Number 2. 2012.

[17] Liu X.-H, Liu F.-S, Zhou L, Sun B.-G, Schock H. J. Backfire prediction in a manifold injection hydrogen internal combustion engine. Int J Hydrogen Energy, 2008. 33(14): p. 3847-3855.

[18] Abele A. Quantum hydrogen prius, in ARB ZEV Technology Symposium. 2006: Sacramento, California.

[19] Verhelst S, Wallner T. Hydrogen-fueled internal combustion engines. Progress in Energy and Combustion Science, 2009. 35(6): p. 490-527.

[20] T. Wallner, H. Lohse-Busch, S. Gurski, M. Duoba, W. Thiel, D. Martin, and T. Korn, Fuel economy and emissions evaluation of a BMW hydrogen 7 mono-fuel demonstration vehicle, Int J. Hydrogen Energy, 2008. 33(24):, p. 7607–7618.

[21] Heller K, Ellgas S. Optimization of hydrogen internal combustion engine with cryogenic mixture formation. presented at the 1st Int Symp on Hydrogen Internal Combustion Engines, Graz, Austria, Sept. 28-29, 2006, pp. 49-58.

[22] K. Yamane, M. Nogami, Y. Umemura, M. Oikawa, Y. Sato, Y. Goto “Development of High Pressure H_2 Gas Injectors, Capable of Injection at Large Injection Rate and High Response Using a Common-rail Type Actuating System for a 4-cylinder, 4.7-liter Total Displacement, Spark Ignition Hydrogen Engine” SAE paper 2011-01-2005, 2011

[23] D. Mumford, A. Welch, B. Bartunek: “Development of H_2 Direct Injection Technology for High Efficiency / High BMEP Engines”, 1st International Symposium on Hydrogen Internal Combustion Engines, September 28-29, 2006, Graz, Austria.

[24] A. Welch, D. Mumford, S. Munshi, J. Holbery, B. Boyer, M. Younkins, H. Jung, “Challenges in Developing Hydrogen Direct Injection Technology for Internal Combustion Engines”, SAE paper 2008-01-2379.

[25] P. Steinrueck, G. Ranegger, “Timed Injection of Hydrogen for Fuel Cells and Internal Combustion Engines”, 1st International Symposium on Hydrogen Internal Combustion Engines, September 28-29, 2006, Graz, Austria.

[26] R. Scarcelli, T. Wallner, V.M. Salazar, S.A. Kaiser, "CFD and Optical Investigations of Fluid Dynamics and Mixture Formation in a DI-H_2ICE", ICEF2010-35084, ASME 2010 Internal Combustion Engines Division Fall Technical Conference (ICEF), San Antonio, TX, USA, September 12-15, 2010.

[27] R.Scarcelli, T. Wallner, N. Matthias, V, Salazar, S. Kaiser, “Mixture Formation in Direct Injection Hydrogen Engines: CFD and Optical Analysis of Single- and Multi-Hole Nozzles”, SAE International Journal of Engines, August 2011, vol. 4, no. 2, 2361-2375, 2011.

[28] D.J. Tritton, Physical Fluid Dynamics, Section 22.7, “The Coanda Effect”,Van Nostrand Reinhold, 1977 (reprinted 1980).

[29] Heindl R, Eichlseder H, Spuller C, Gerbig F, Heller K. New and Innovative Combustion Systems for H_2-ICE: Compression Ignition and Combined Processes. SAE paper 2009-01-1421.

[30] Tanno S, Ito Y, Michikawauchi R, Nakamura M, Tomita H. High-Efficiency and Low-NOx Hydrogen Combustion by High Pressure Direct Injection. SAE paper 2010-01-2173.

[31] Matthias NS, Wallner T, Scarcelli R. A Hydrogen Direct Injection Engine Concept that Exceeds U.S. DOE Light-Duty Efficiency Targets. SAE paper 2012-01-0653.

[32] Wimmer A, Wallner T, Ringler J, Gerbig F. H_2-Direct Injection: a Highly Promising Combustion Concept. SAE paper 2005-01-0108.

[33] Eichlseder H, Grabner G, Gerbig F, Heller K. Advanced Combustion Concepts and Development Methods for Hydrogen IC Engines. FISITA 2008 World Automotive Congress. 2008. Munich, Germany.

[34] Michl J, Schenk M, Rottengruber H, Huhn W. Thermal Boundary Conditions in a Stoichiometric Operating Hydrogen Engine. FISITA 2008 World Automotive Congress. 2008. Munich, Germany.

[35] Shudo T, Nabetani S. Analysis of Degree of Constant Volume and cooling Loss in a Hydrogen Fuelled SI Engine. SAE paper 2001-01-3561.

[36] Shudo T. Improving thermal efficiency by reducing cooling losses in hydrogen combustion engines. International Journal of Hydrogen Energy, 2007. 32(17): p. 4285-4293.

[37] Shudo T, Nakajima Y, Futakuchi T. Thermal efficiency analysis in a hydrogen premixed combustion engine. JSAE Review, 2000. 21(2): p. 177-182.

[38] Wei S. A Study on Transient Heat Transfer Coefficient of In-cylinder Gas in the Hydrogen Fueled Engine. in KHES and HESS, the 6th Korea-Japan Joint Symposium on Hydrogen Energy. 2001.

[39] Demuynck J, De Paepe M, Huisseune H, Vancoillie J, Sierens R, Verhelst S. Investigation Of The Influence Of Engine Settings On The Heat Flux In A Hydrogen- And Methane-Fuelled Spark Ignition Engine. Applied Thermal Engineering, 2011. 31: p. 1220-1228.

[40] Demuynck J, De Paepe M, Huisseune H, Sierens R, Vancoillie J, Verhelst S. On the applicability of empirical heat transfer models for hydrogen combustion engines. International Journal of Hydrogen Energy, 2011. 36(1): p. 975-984.

[41] Shudo T, Suzuki H. Applicability of heat transfer equations to hydrogen combustion. JSAE Review, 2002. 23(3): p. 303-308.

[42] Pischinger R, Klell M, Sams T.Thermodynamik der Verbrennungskraftmaschine. Springer Verlag. 2002.

[43] Rousseau A, Wallner T, Pagerit S, Lohse-Busch H. Prospects on Fuel Economy Improvements for Hydrogen Powered Vehicles. SAE paper 2008-01-2378.

[44] Wallner T, Matthias NS, Scarcelli R, Kwon JC. “Evaluation of Efficiency and Drive Cycle Emissions for a Hydrogen Direct Injection Engine” Proceedings of the IMechE Part D Journal of Automobile Engineering, special issue on Vehicle Fuel Economy: High Efficiency Engines and Hybrid Powertrains, 2012.

[45] DieselNet. “Emissions Standards: USA: Cars and Light-Duty Trucks – Tier 2”. Retrieved 5/4/2011: http://www.dieselnet.com/standards/us/ld_t2.php

[46] U.S. Department of Energy office of Energy Efficiency and Renewable Energy. “Vehicle Technologies Program Multi-Year Program Plan 2011-2015”. Retrieved 5/4/2011: http://www1.eere.energy.gov/vehiclesandfuels/pdfs/program/vt_mypp_2011-2015.pdf

Figure captions

Figure 1: Comparison of flammability limits of typical engine fuels

Figure 18: Efficiency analysis at low and high load points [31]

Figure 19: Fuel economy and emissions behavior of a simulated hydrogen DI engine vehicle [44]

Table 1: Properties of hydrogen compared to methane and iso-octane

Property	Hydrogen	Methane	Iso-octane
Molecular weight [g/mol]	2.016	16.043	114.236
Density gaseous [kg/m3]	0.08	0.65	-
Density liquefied [kg/m3]	71	430-470	692
Minimum ignition energy [mJ]	0.02	0.28	0.28
Minimum quenching distance [mm]	0.64	2.03	3.5
Lower heating value [MJ/kg]	120	50	44.3
Stoichiometric air/fuel ratio [kg/kg]	34.2	17.1	15
Flammability limits in air [vol%]	4-75	5-15	1.1-6
Flammability limits (λ[1]) [-]	10-0.14	2-0.6	1.51-0.26
Flammability limits (φ[2])[-]	0.1-7.1	0.5-1.67	0.66-3.85

Table 2: Characteristics and performance of the examined injectors: EHI [19], EMV and Piezo

Injector	EHI	EMV	Piezo
Control method	ON/OFF	ON/OFF	Analog
Maximum Injection pressure [bar]	200	150	250
Maximum Needle Lift [mm]	0.87	0.25	0.1
Start of injection (SOI) delay [ms]	0.375	0.3	0.05
Opening transient duration [ms]	1.42	0.4	0.5
Rate of needle lift during opening [m/s]	0.61	0.62	0.2
Average Mass Flow Rate at 100 bar [g/s]	5.91	2.24	3.94
Average Mass Flux at 100 bar [kg/m^2·s]	1607	1750	5184
Maximum Mass Flow Rate at 100 bar [g/s]	10.25	2.93	6.22
Mass Flow Rate Increase during transient [g/s·CAD]	0.79	0.73	1.24

Table 3 The effect of the heat loss is reflected in the indicated efficiency, which drops from 29 to 23% for hydrogen going from low to high load

Fuel	Ignition [°CA BTDC]	λ	Throttle	W_i [J]	IMEP [bar]	ITE [%]	Heat loss [J]	Heat loss [%]
Hydrogen	4	2	WOT	287	4.7	29	235	24
Methane	23	1	77°	294	4.8	25	343	29
Hydrogen	-2	1.5	WOT	327	5.3	26	353	28
Methane	23	1	76°	317	5.2	25	329	26
Hydrogen	-6	1	WOT	376	6.1	23	597	37
Methane	23	1	74°	367	6	26	386	27

[1] relative air/fuel ratio
[2] fuel/air equivalence ratio

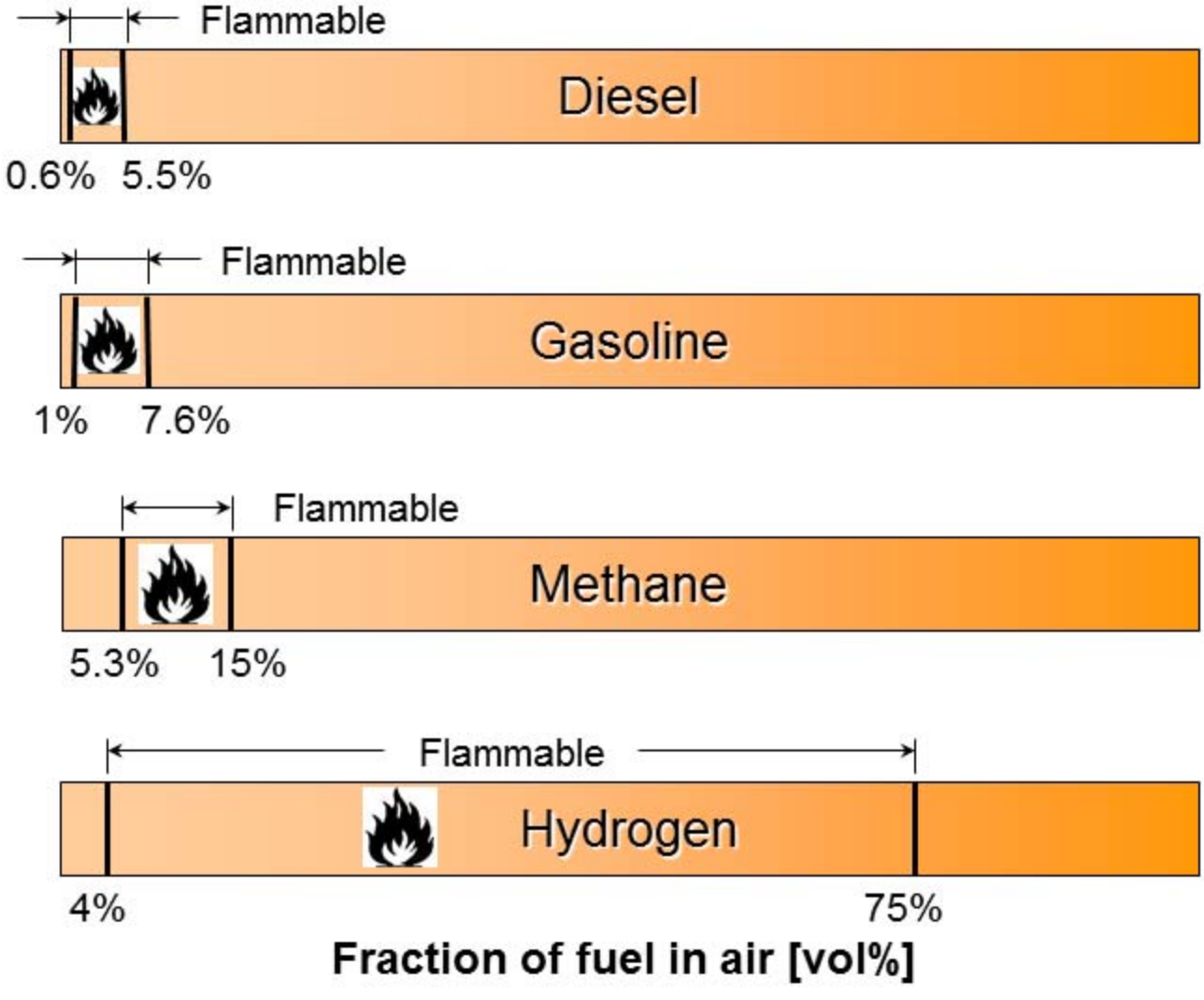
Flammable
Diesel
0.6%
5.5%
Flammable
Gasoline
1%
7.6%
Flammable
Methane
5.3%
15%
Flammable
Hydrogen
4%
75%
Fraction of fuel in air [vol%]

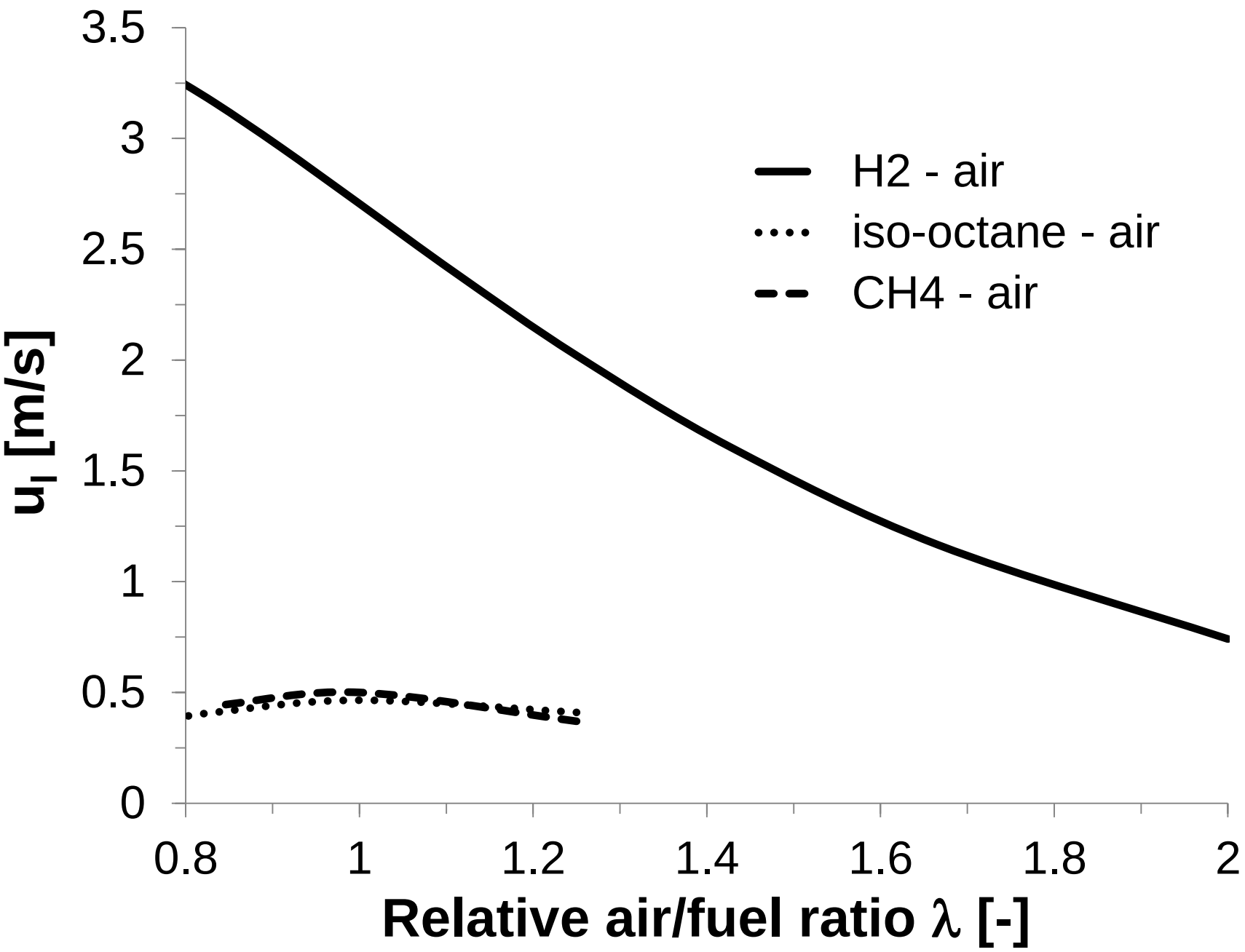
3.5
3
2.5
2
1.5
1
0.5
0
u_l [m/s]
0.8
1
1.2
1.4
1.6
1.8
2
Relative air/fuel ratio λ [-]
H2 - air
iso-octane - air
CH4 - air

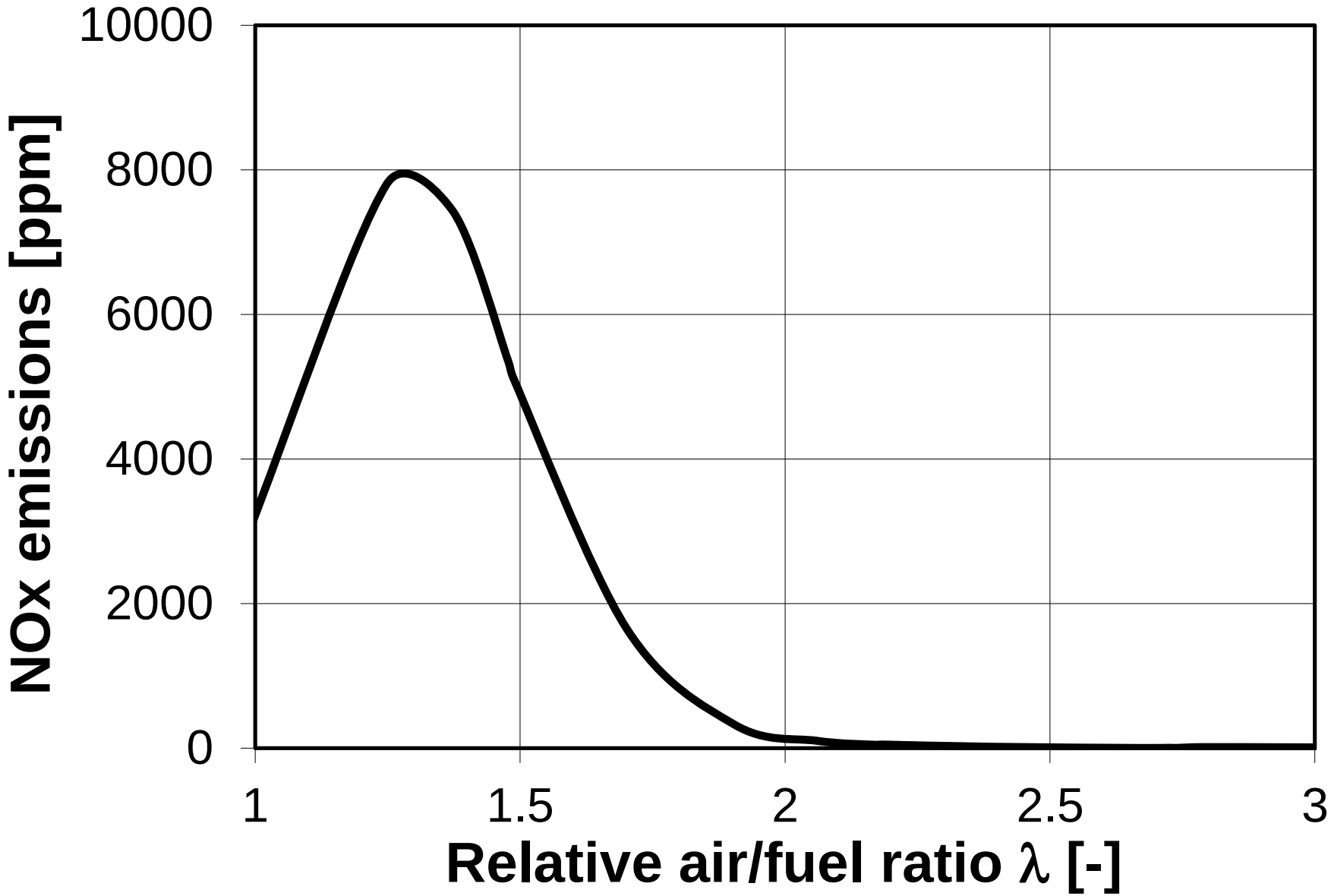
10000
8000
6000
4000
2000
0
NOx emissions [ppm]
1
1.5
2
2.5
3
Relative air/fuel ratio λ [-]

Assumptions:

λ=1
λ_a=const.
η_e=const.
η=const.
V_H=const.

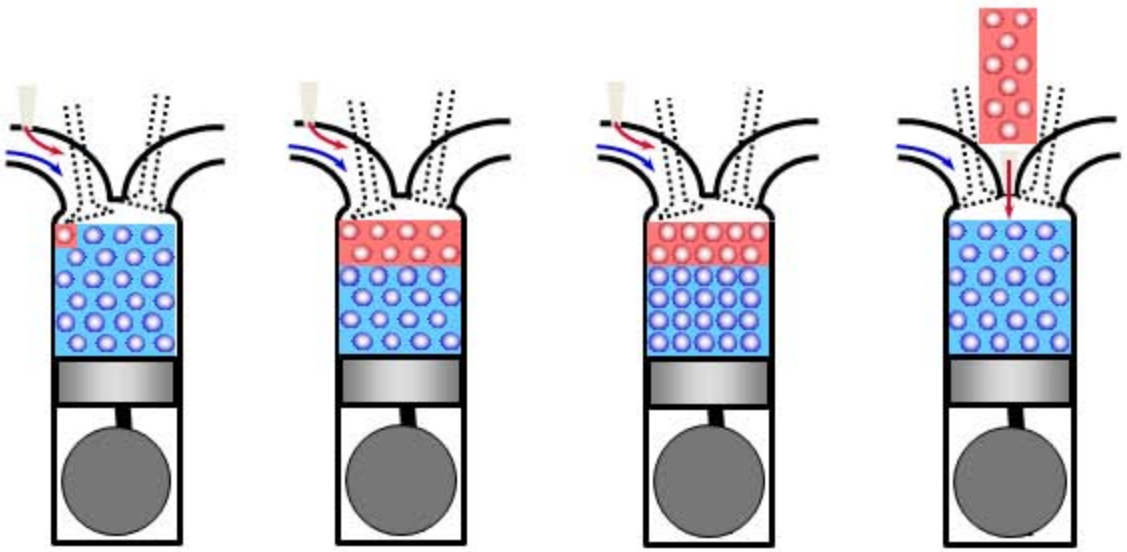

Fuel	**Gasoline**	**Hydrogen**	**Hydrogen**	**Hydrogen**
Mixture formation	Port injection	Port injection	Cryogenic Port injection	Direct injection
Mixture temperature [K]	293	293	210	293
Mixture cal. value [MJ/m³]	3.59	2.97	4.14	4.21
Specific power [%]	**100**	**83**	**115**	**117**

"State-of-the-art" *"Advanced technology"*

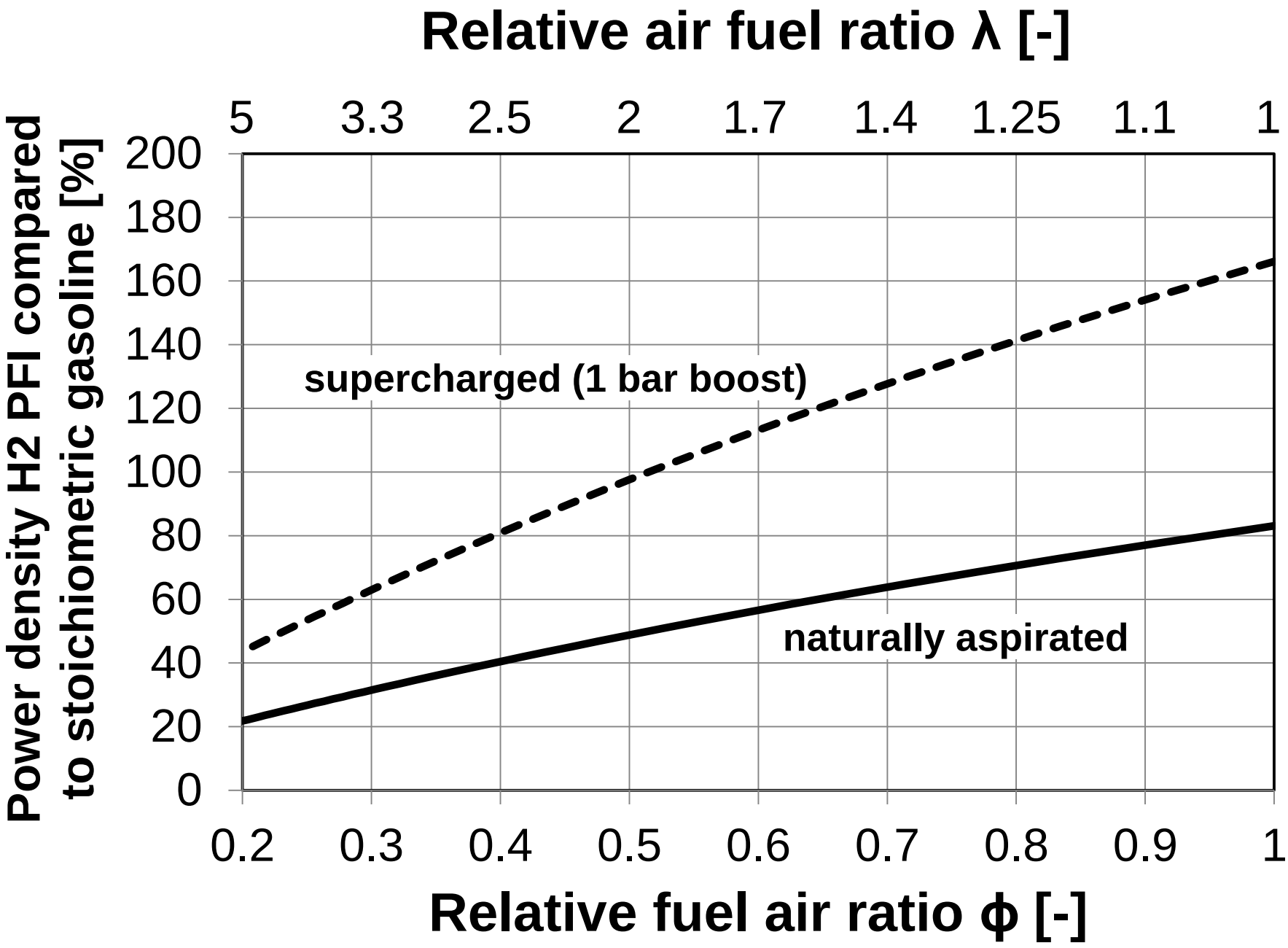
Relative air fuel ratio λ [-]
5
3.3
2.5
2
1.7
1.4
1.25
1.1
1
Power density H2 PFI compared to stoichiometric gasoline [%]
200
180
160
140
120
100
80
60
40
20
0
supercharged (1 bar boost)
naturally aspirated
0.2
0.3
0.4
0.5
0.6
0.7
0.8
0.9
1
Relative fuel air ratio ϕ [-]

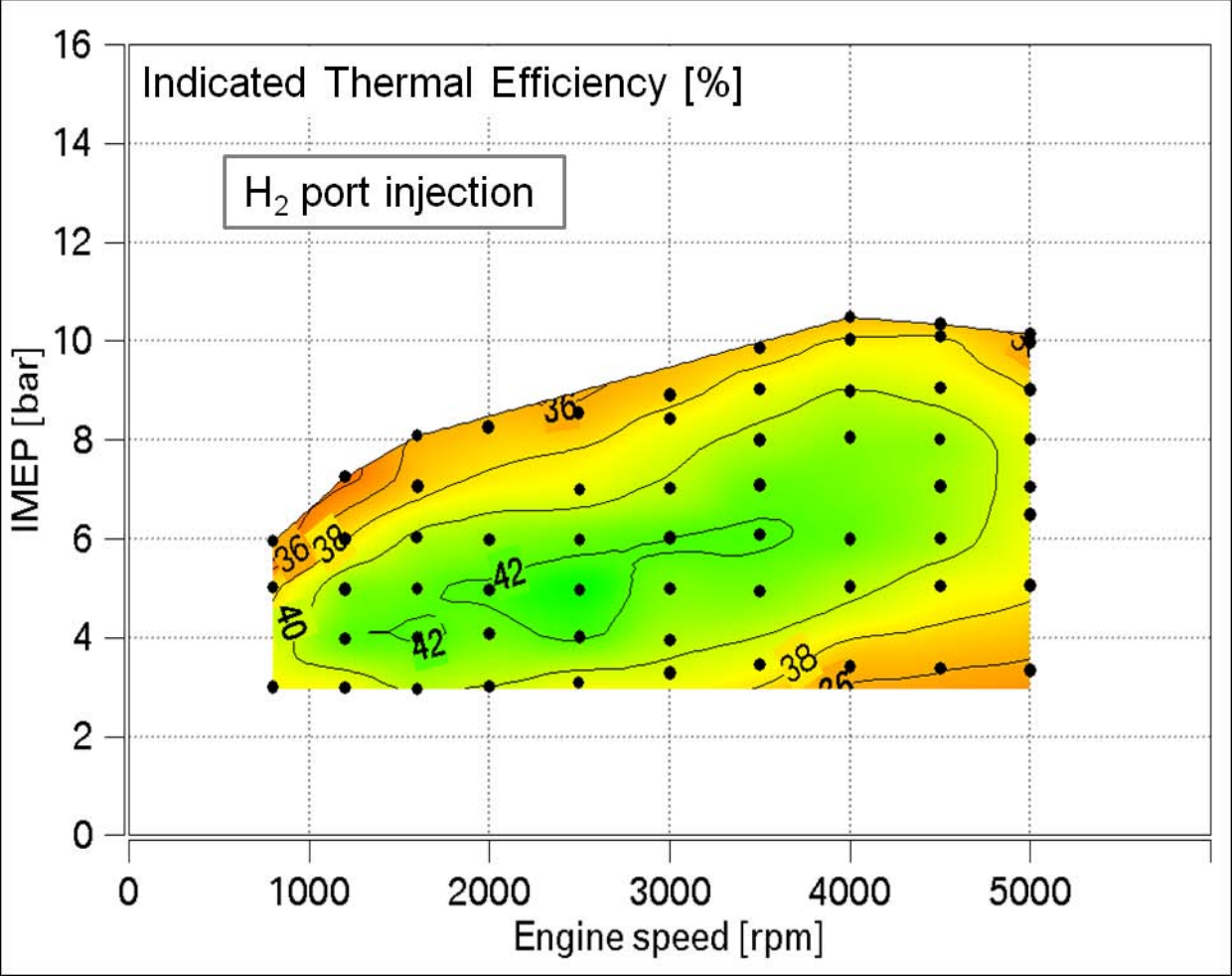
Indicated Thermal Efficiency [%]
H_2 port injection
IMEP [bar]
Engine speed [rpm]
0
2
4
6
8
10
12
14
16
0
1000
2000
3000
4000
5000
36
38
42
40
42
38


Lyse
HYDROGEN


BMW Hydrogen Power
CleanEnergy
Powered by Hydrogen
M HY 7701

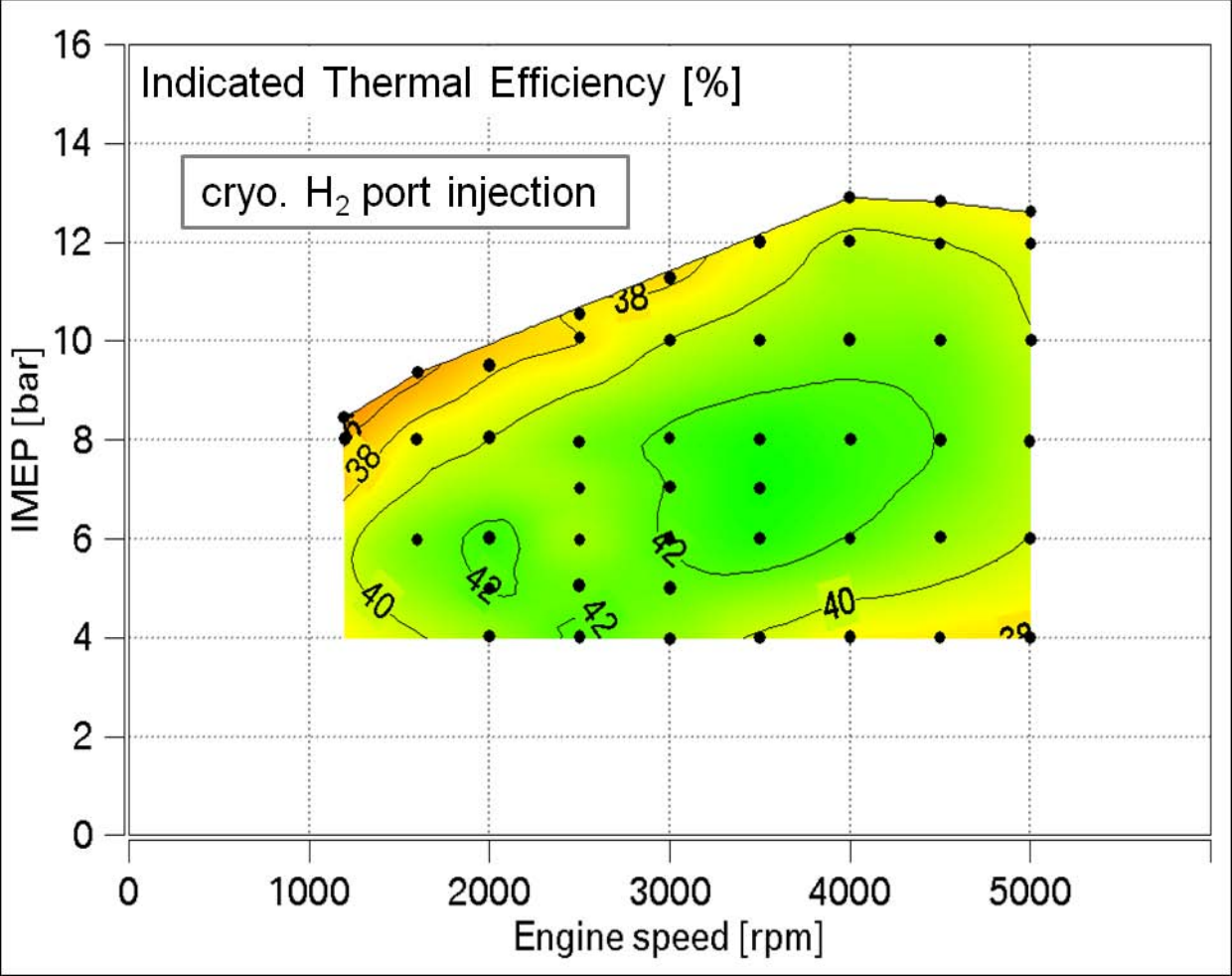
Indicated Thermal Efficiency [%]
cryo. H_2 port injection
38
38
42
42
42
40
40
38
IMEP [bar]
16
14
12
10
8
6
4
2
0
0
1000
2000
3000
4000
5000
Engine speed [rpm]

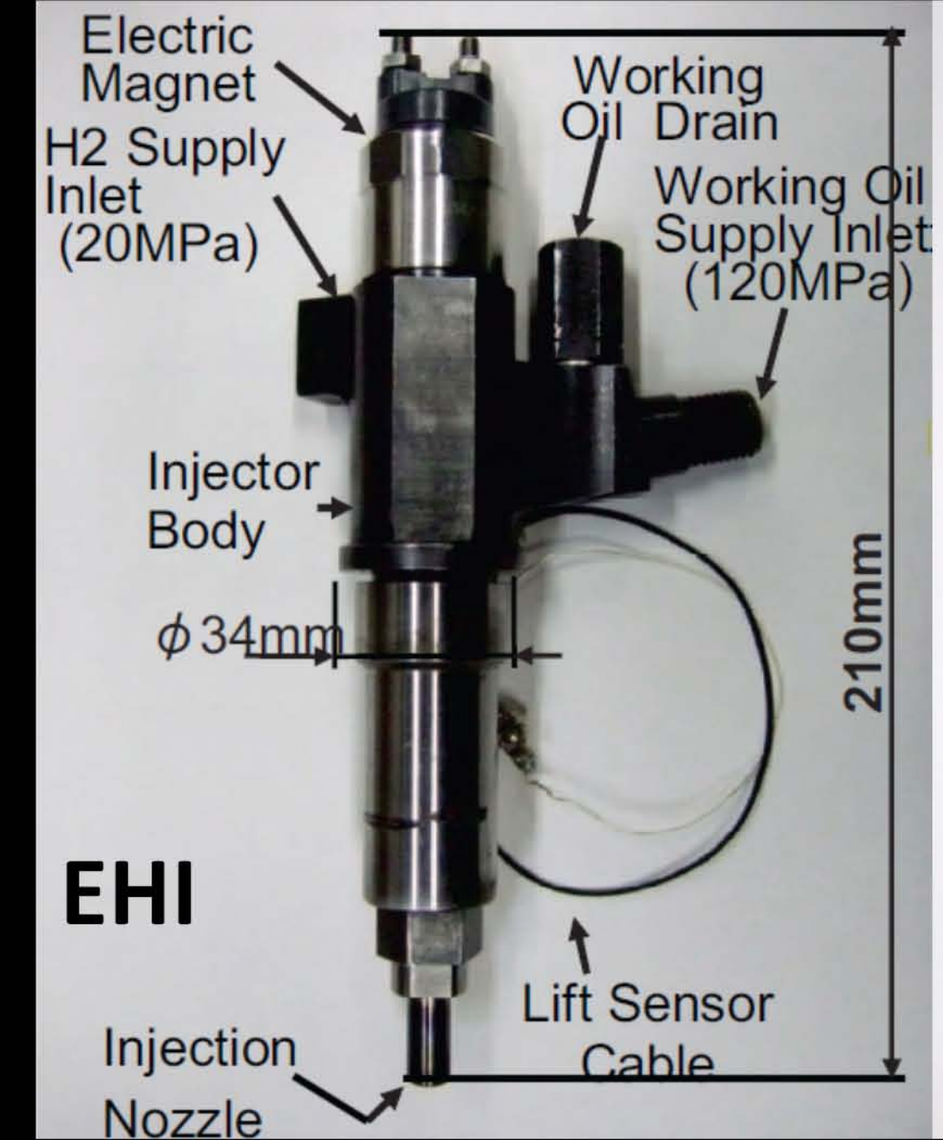
Electric Magnet
H2 Supply Inlet (20MPa)
Working Oil Drain
Working Oil Supply Inlet (120MPa)
Injector Body
ϕ34mm
210mm
Lift Sensor Cable
Injection Nozzle
EHI

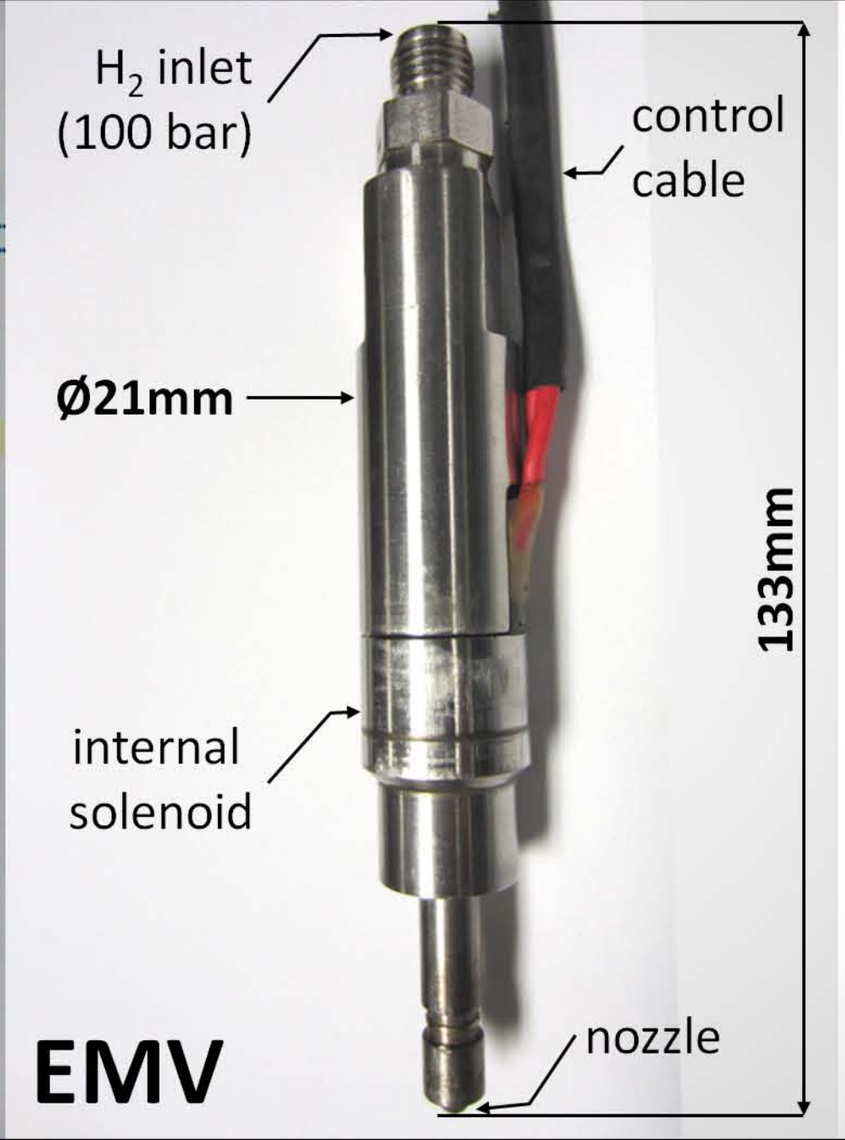
H2 inlet (100 bar)
control cable
Ø21mm
133mm
internal solenoid
nozzle
EMV

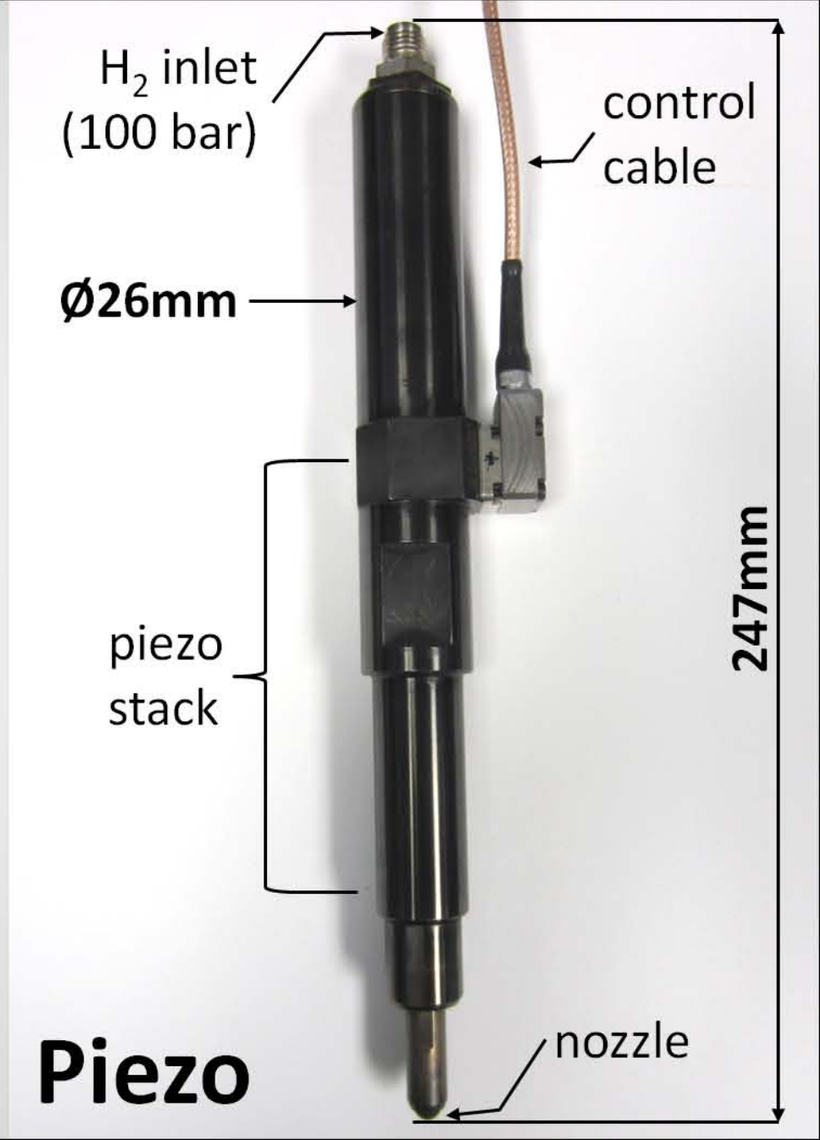
H2 inlet (100 bar)
control cable
Ø26mm
piezo stack
247mm
nozzle
Piezo

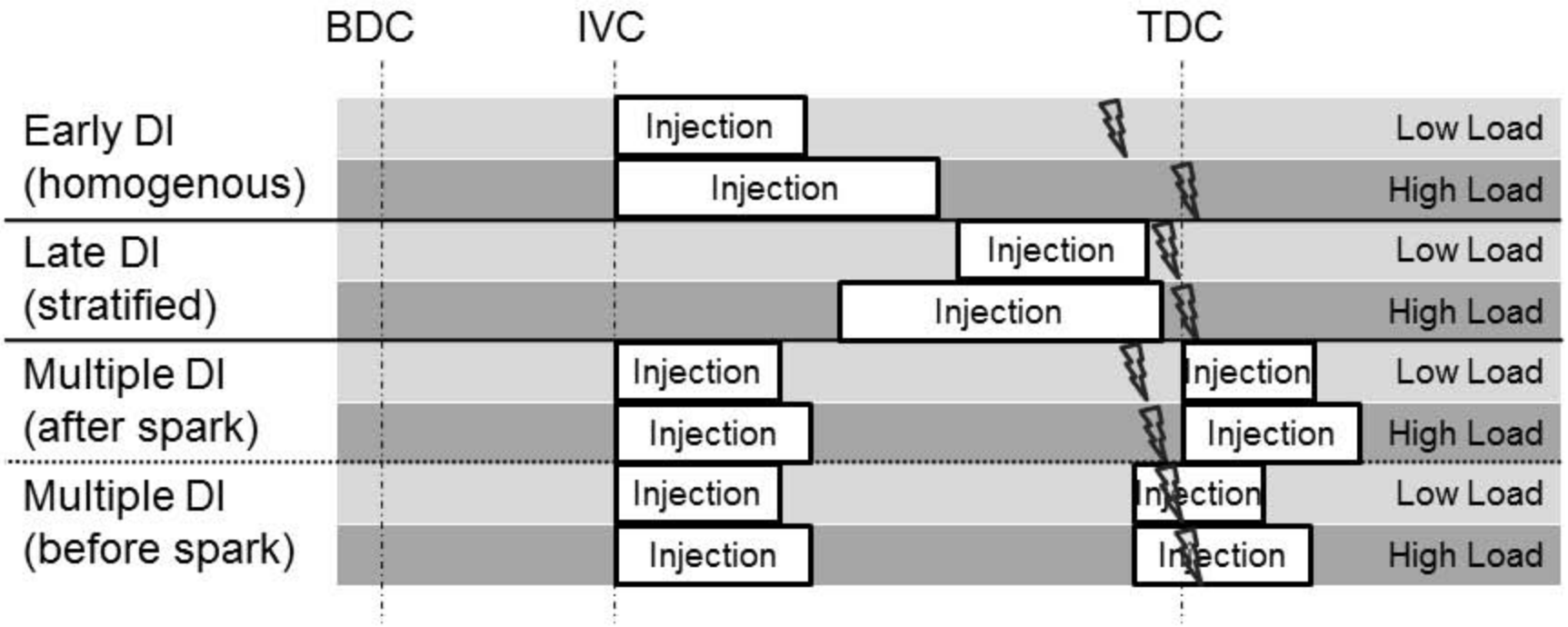
BDC
IVC
TDC
Early DI
(homogenous)
Late DI
(stratified)
Multiple DI
(after spark)
Multiple DI
(before spark)
Injection
Low Load
High Load

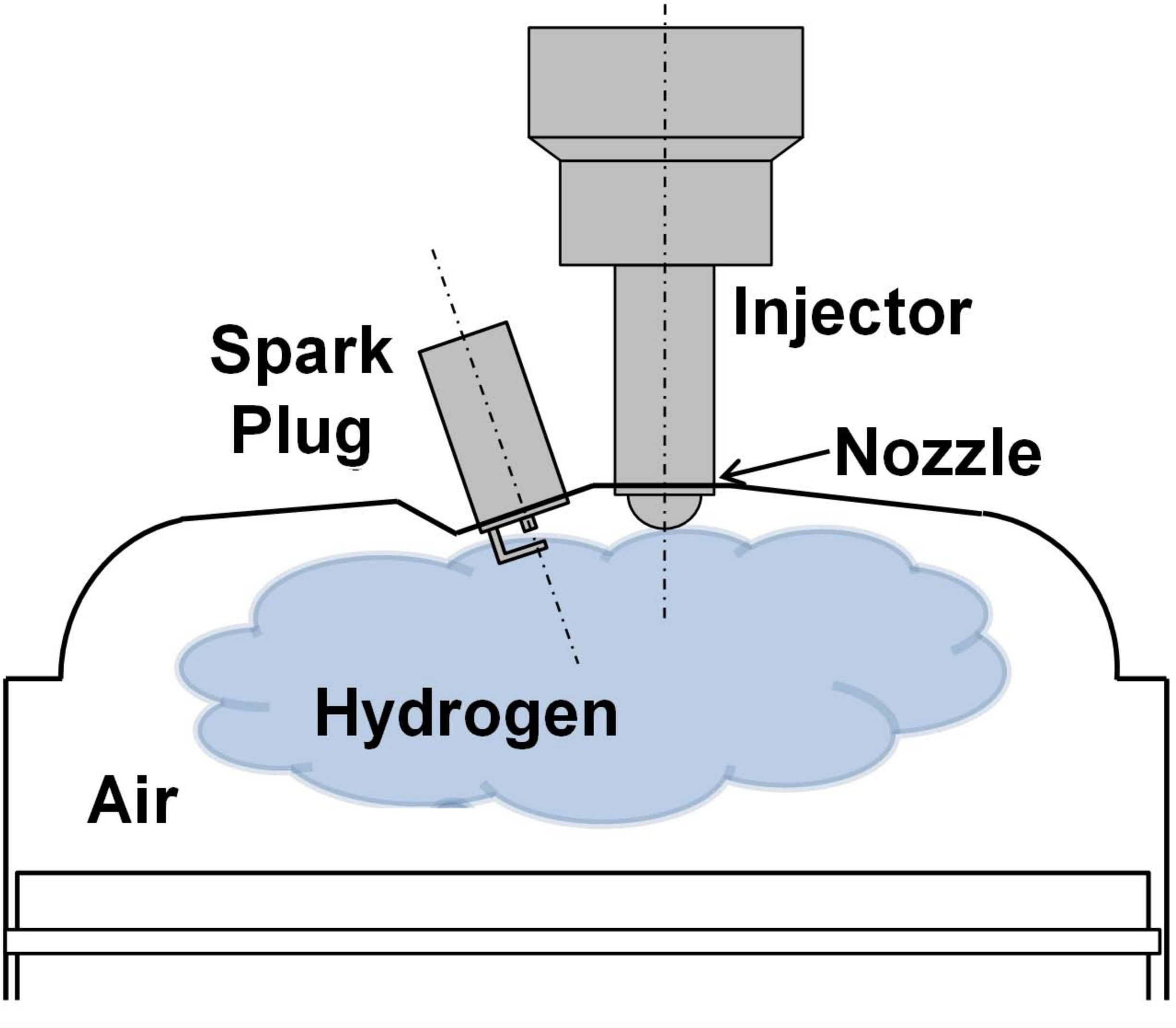
Spark
Plug
Injector
Nozzle
Hydrogen
Air

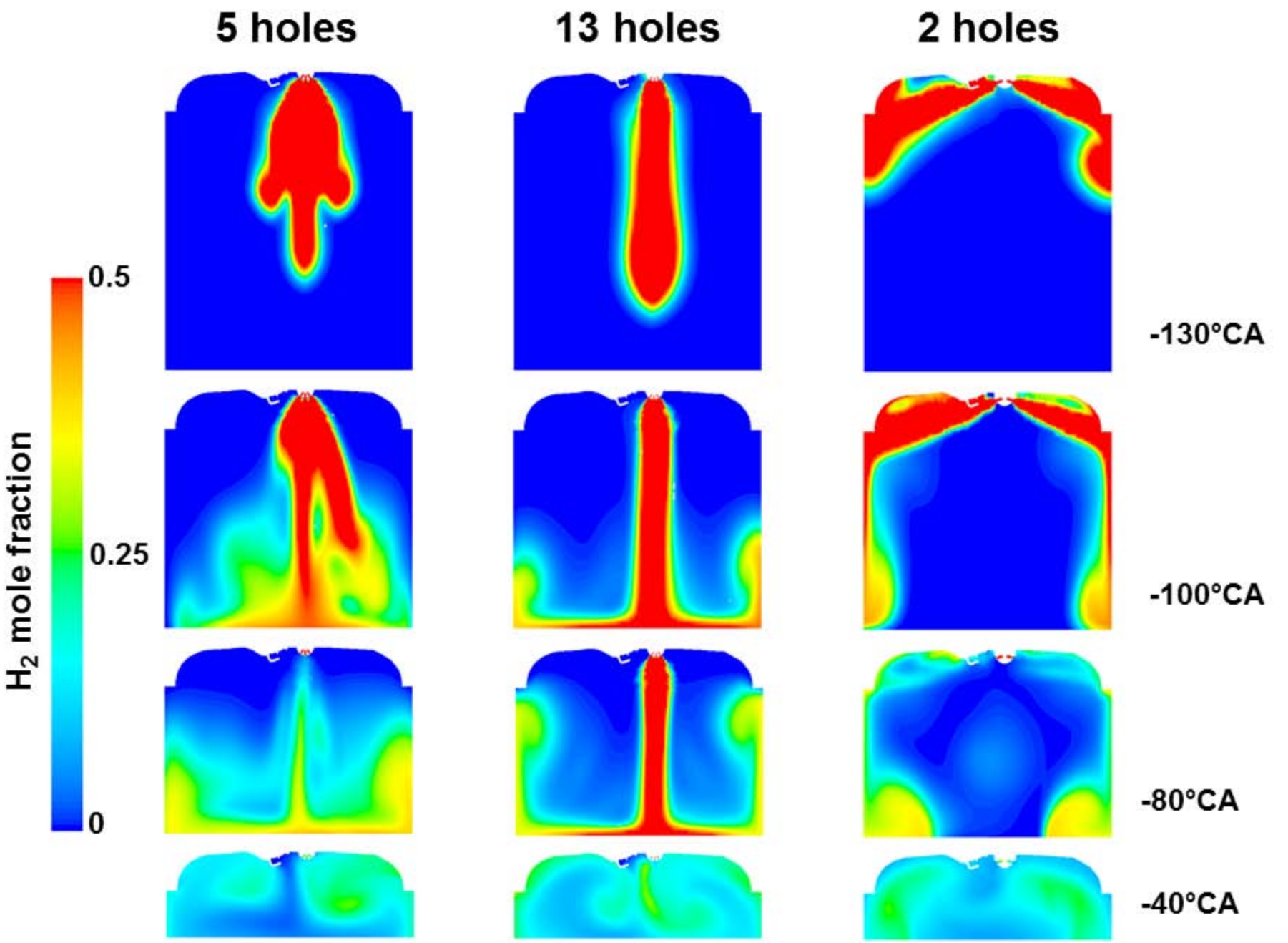
5 holes
13 holes
2 holes
0.5
0.25
0
H_2 mole fraction
-130°CA
-100°CA
-80°CA
-40°CA

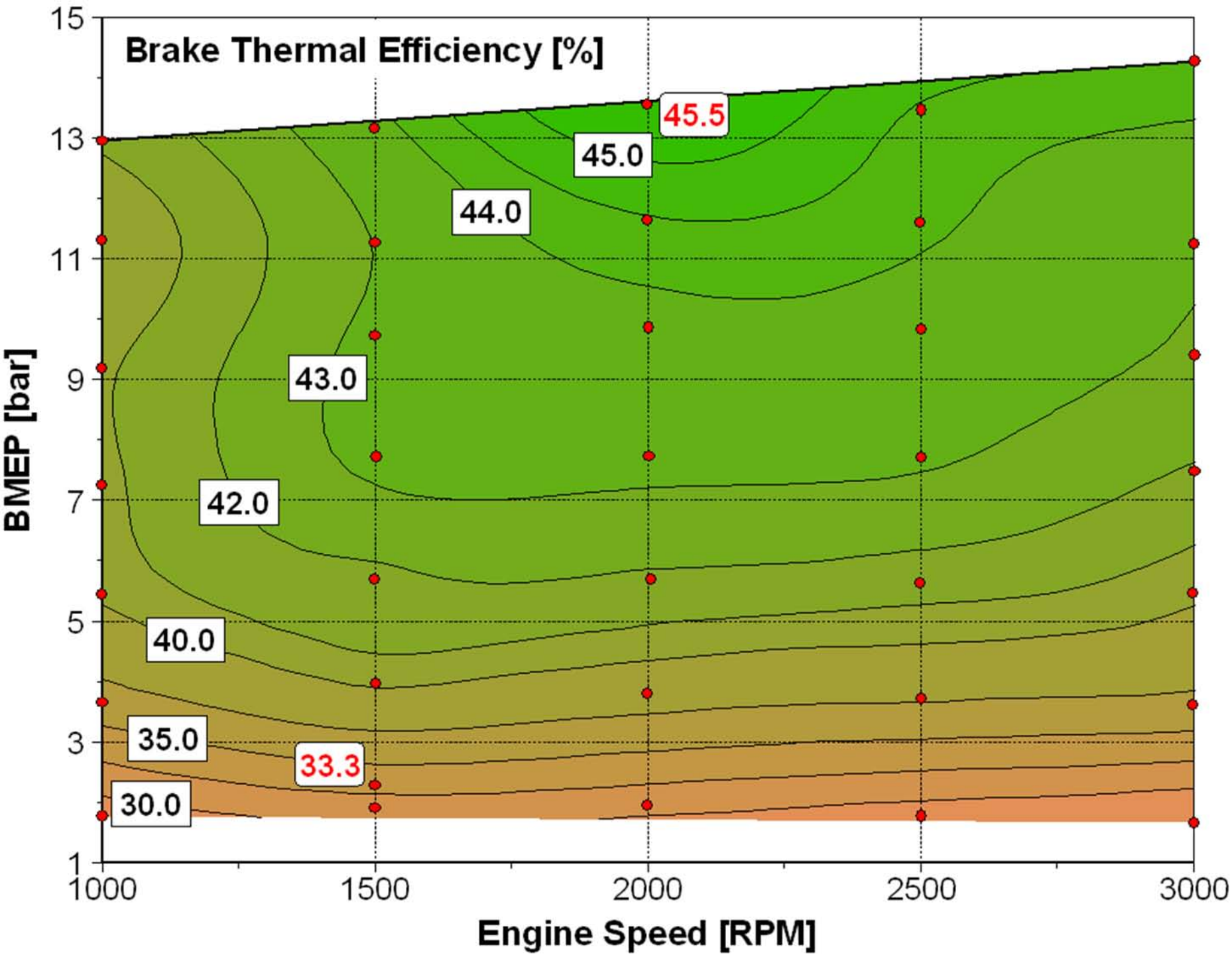
Brake Thermal Efficiency [%]
45.5
45.0
44.0
43.0
42.0
40.0
35.0
33.3
30.0
BMEP [bar]
15
13
11
9
7
5
3
1
1000
1500
2000
2500
3000
Engine Speed [RPM]

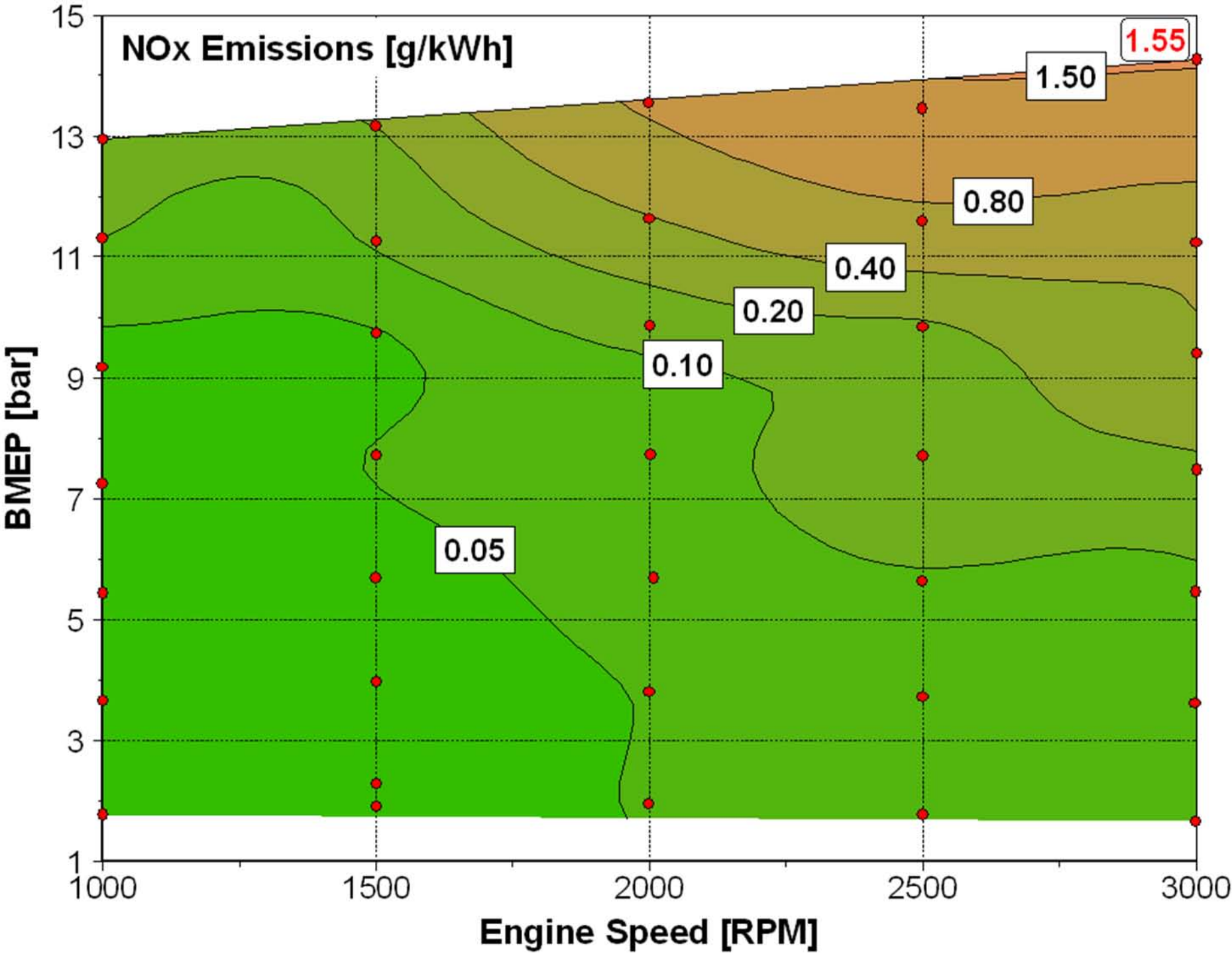
NOx Emissions [g/kWh]
1.55
1.50
0.80
0.40
0.20
0.10
0.05
BMEP [bar]
15
13
11
9
7
5
3
1
1000
1500
2000
2500
3000
Engine Speed [RPM]

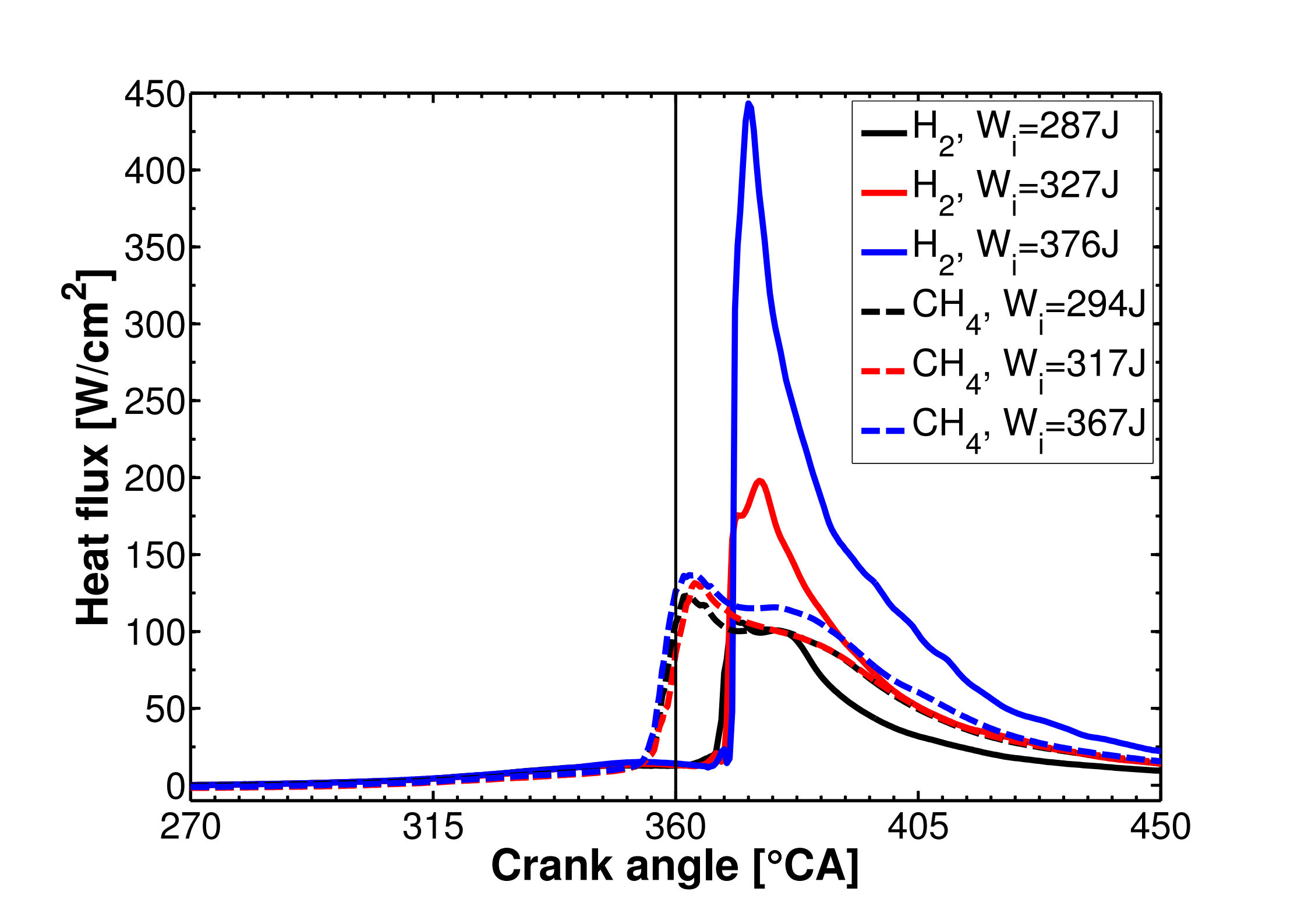
Heat flux [W/cm^2]
Crank angle [°CA]
450
400
350
300
250
200
150
100
50
0
270
315
360
405
450
H$_2$, W$_i$=287J
H$_2$, W$_i$=327J
H$_2$, W$_i$=376J
CH$_4$, W$_i$=294J
CH$_4$, W$_i$=317J
CH$_4$, W$_i$=367J

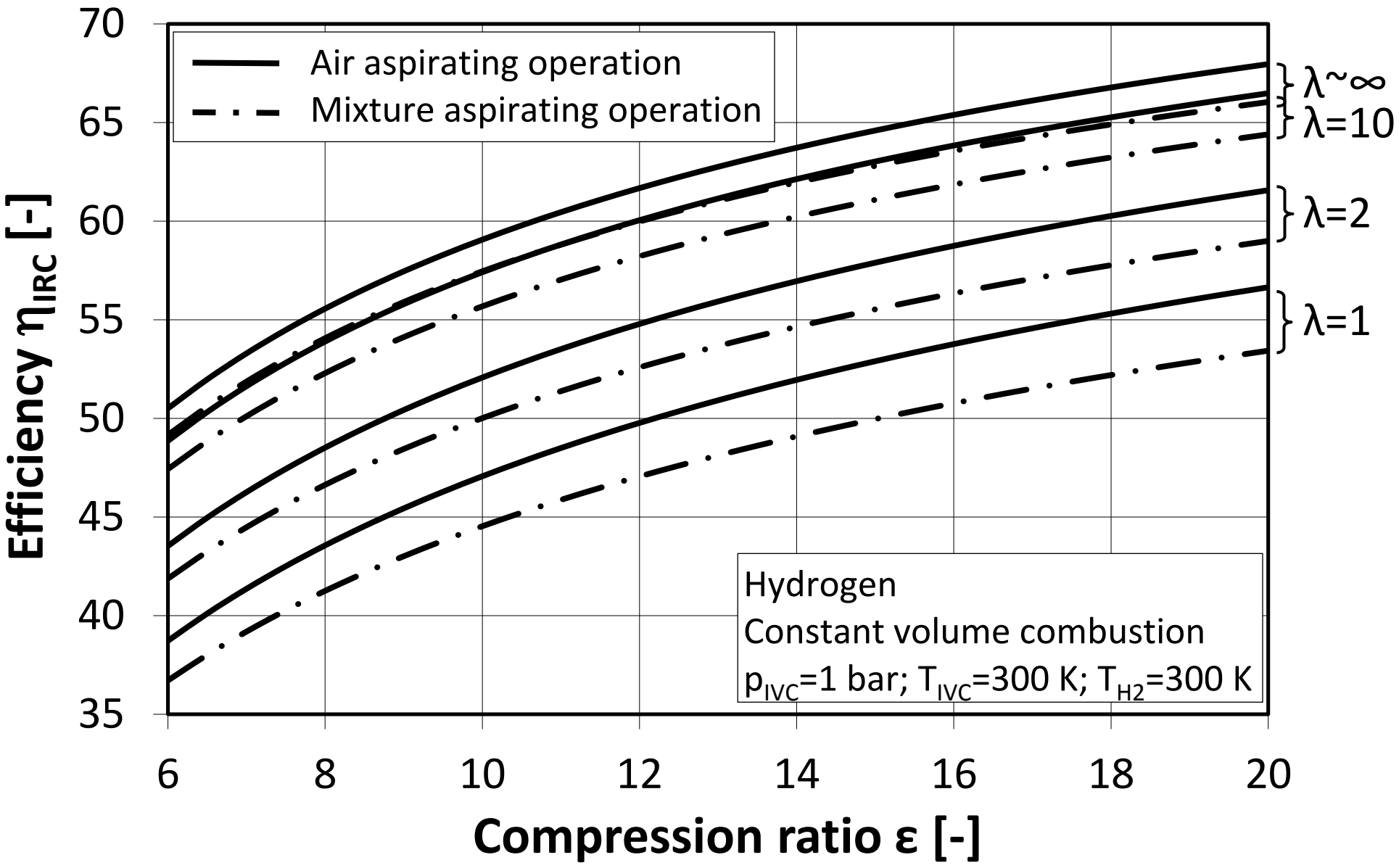
Air aspirating operation
Mixture aspirating operation
λ~∞
λ=10
λ=2
λ=1
Hydrogen
Constant volume combustion
p_{IVC}=1 bar; T_{IVC}=300 K; T_{H2}=300 K
Efficiency η_{IRC} [-]
Compression ratio ε [-]
70
65
60
55
50
45
40
35
6
8
10
12
14
16
18
20

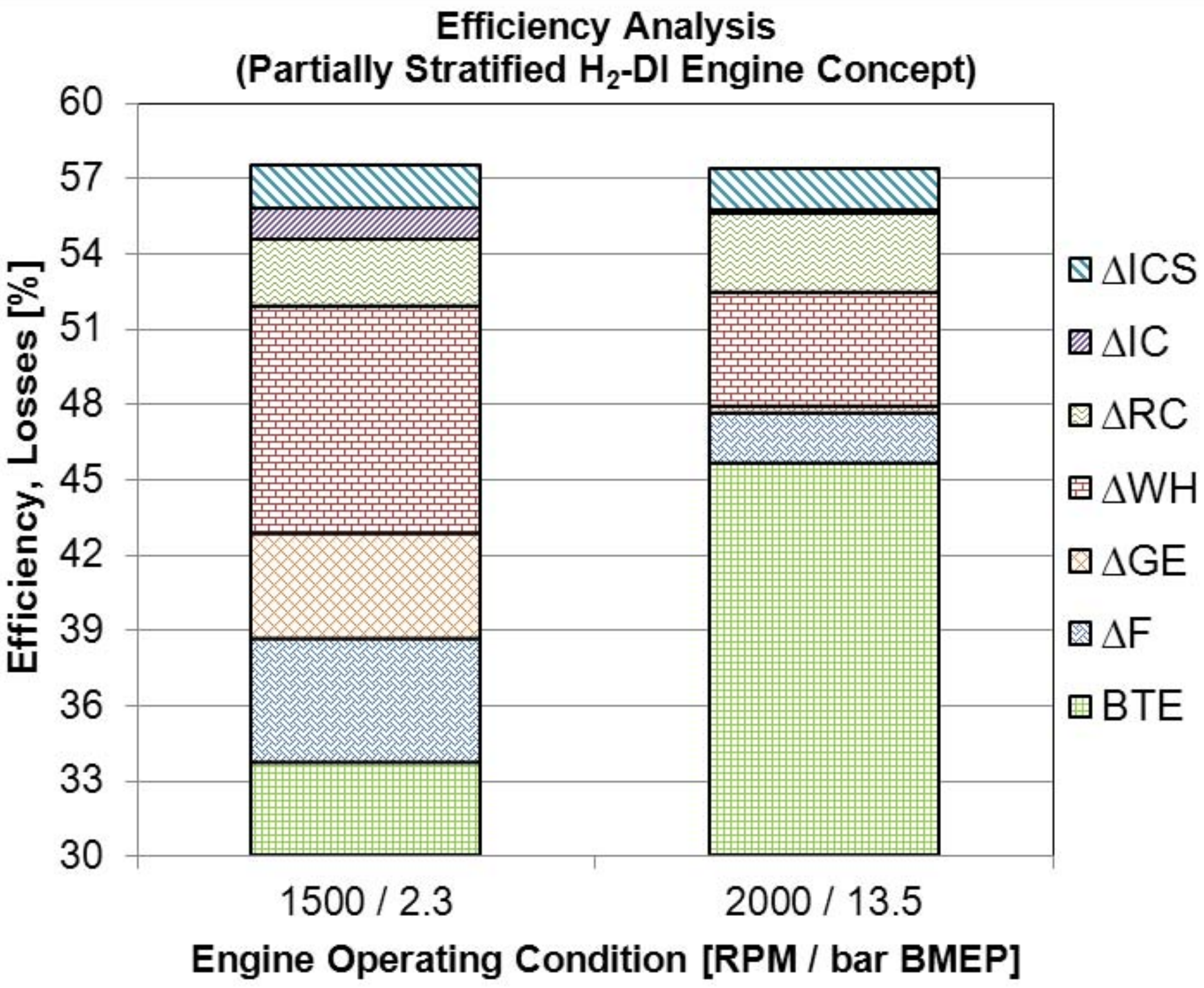
Efficiency Analysis
(Partially Stratified H2-DI Engine Concept)
60
57
54
51
48
45
42
39
36
33
30
Efficiency, Losses [%]
ΔICS
ΔIC
ΔRC
ΔWH
ΔGE
ΔF
BTE
1500 / 2.3
2000 / 13.5
Engine Operating Condition [RPM / bar BMEP]

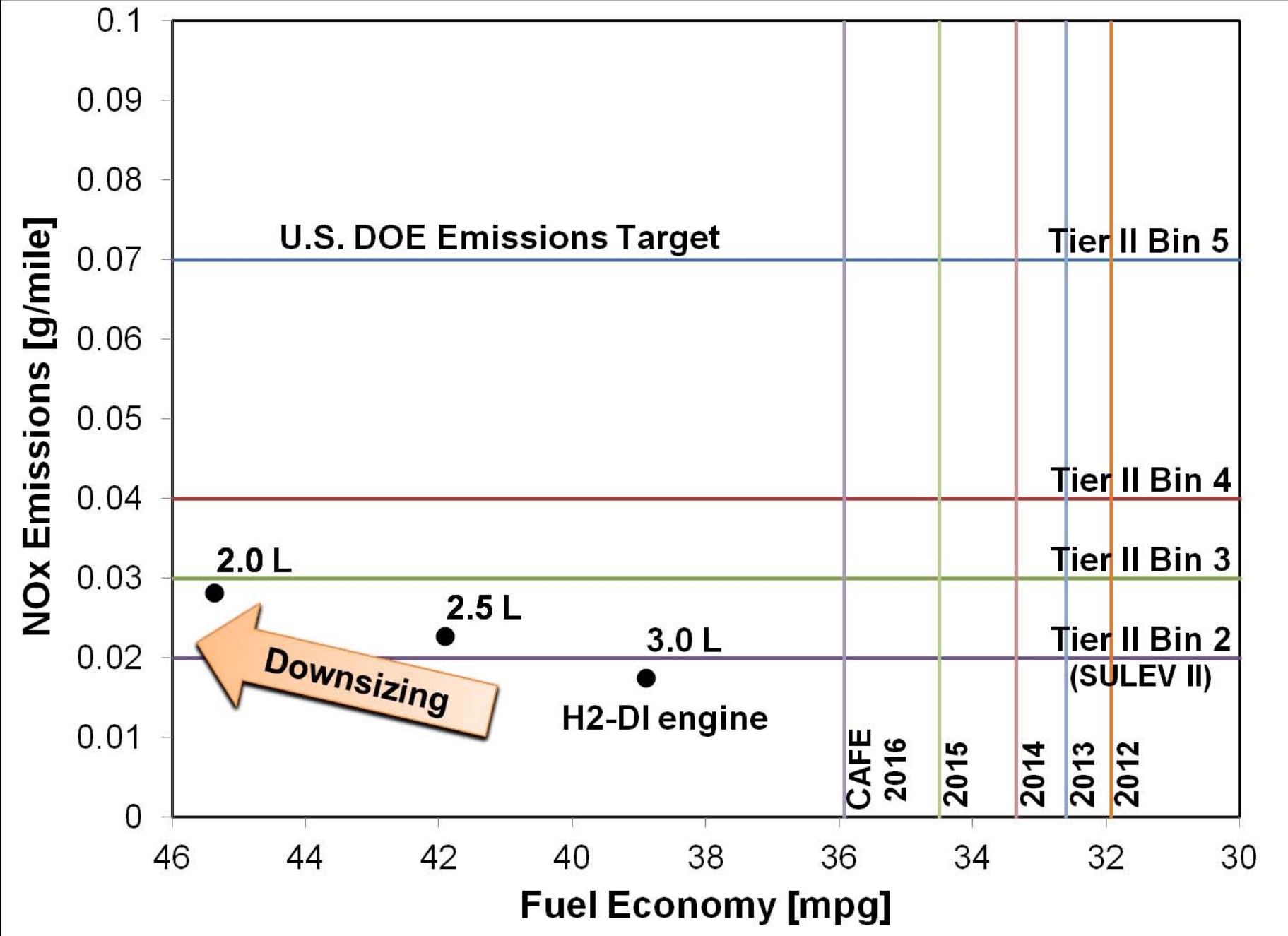
0.1
0.09
0.08
0.07
0.06
0.05
0.04
0.03
0.02
0.01
0
NOx Emissions [g/mile]
U.S. DOE Emissions Target
Tier II Bin 5
Tier II Bin 4
Tier II Bin 3
Tier II Bin 2
(SULEV II)
2.0 L
2.5 L
3.0 L
Downsizing
H2-DI engine
CAFE 2016
2015
2014
2013
2012
46
44
42
40
38
36
34
32
30
Fuel Economy [mpg]